

**FORN
H
AZ
R
O
U
M**

DOE/ET/10145-74

Vol. 1 of 2

**DATA REQUIREMENTS FOR EOR SURFACTANT-POLYMER
PROCESS SIMULATION AND ANALYSIS OF EL DORADO
PILOT PROJECT SIMULATION, BUTLER COUNTY, KANSAS**

Vol. I: Technical Report

Work Performed for the Department of Energy
Under Contract No. DE-AC01-78ET10145

Date Published—January 1983

Gulf Universities Research Consortium
Bellaire, Texas



U. S. DEPARTMENT OF ENERGY

DISCLAIMER

This report was prepared as an account of work sponsored by an agency of the United States Government. Neither the United States Government nor any agency thereof, nor any of their employees, makes any warranty, express or implied, or assumes any legal liability or responsibility for the accuracy, completeness, or usefulness of any information, apparatus, product, or process disclosed, or represents that its use would not infringe privately owned rights. Reference herein to any specific commercial product, process, or service by trade name, trademark, manufacturer, or otherwise, does not necessarily constitute or imply its endorsement, recommendation, or favoring by the United States Government or any agency thereof. The views and opinions of authors expressed herein do not necessarily state or reflect those of the United States Government or any agency thereof.

Printed in the United States of America. Available from:
National Technical Information Service
U.S. Department of Commerce
5285 Port Royal Road
Springfield, VA 22161

NTIS price codes
Paper copy: \$9.00
Microfiche copy: \$4.00

**DATA REQUIREMENTS FOR EOR SURFACTANT-POLYMER
PROCESS SIMULATION AND ANALYSIS OF EL DORADO
PILOT PROJECT SIMULATION, BUTLER COUNTY, KANSAS**

Vol. I: Technical Report

By

E. L. Claridge and A. Lohse

James L. Gumnick, *Principal Investigator*
Gulf Universities Research Consortium
5909 West Loop South, Suite 600
Bellaire, Texas 77401

Fred W. Burch, *Technical Project Officer*
Bartlesville Energy Technology Center
P.O. Box 1398
Bartlesville, Oklahoma 74005

Work Performed for the Department of Energy
Under Contract No. DE-AC01-78ET10145

Date Published—January 1983

UNITED STATES DEPARTMENT OF ENERGY

TABLE OF CONTENTS

	<u>Page</u>
ACKNOWLEDGEMENTS.....	v
ABSTRACT	vi
1.0 INTRODUCTION	1
1.1 Purpose	1
1.2 Subject of Study	1
1.3 Simulation Strategy	2
2.0 SIMULATION PROBLEMS IN EOR CHEMICAL PROCESSES	4
3.0 SIMULATION FLOW CHART FOR SURFACTANT- POLYMER PROCESS	6
4.0 DATA REQUIREMENTS	8
4.1 Introduction	8
4.2 Geologic Characterization	9
4.2.1 Rock Descriptors	13
4.2.2 Interwell Descriptors	15
4.2.3 Intrasystem Descriptors	17
4.3 Reservoir Characterization	18
4.3.1 Fluid/Rock Descriptors	18
4.3.2 Production Descriptors	24
4.3.3 Flow Rate Descriptors	25
4.4 Process Characterization	25
4.4.1 Introduction	25
4.4.2 Properties Descriptors	27
4.4.3 Interaction Descriptors	28
4.4.4 Function Descriptors	29
5.0 ANALYSIS OF EL DORADO SIMULATION	31
5.1 Introduction	31
5.2 Geologic Characterization	31
5.3 Reservoir Characterization	35
5.3.1 Fluid/Rock Descriptors	35
5.3.2 Production Descriptors	41
5.3.3 Flow Rate Descriptors	41
5.4 Process Characterization	42
5.4.1 Properties Descriptors	42
5.4.2 Interaction Descriptors	44
5.4.3 Coreflood Performance	50

TABLE OF CONTENTS (Concluded)

	<u>Page</u>
6.0 SUMMARY	53
REFERENCES CITED	55
GLOSSARY	58
APPENDIX I	
Process Specific Flow Chart, Evaluation of Surfactant- Polymer Process Simulation, Enhanced Oil Recovery	
APPENDIX II	
El Dorado (High-Water-Content Process) Micellar-Polymer Pilot, Data Assessment and Numerical Simulation	
APPENDIX III	
El Dorado (High-Water-Content Process) Micellar-Polymer Pilot, Appendices to Final Report	

FIGURES

	<u>Page</u>
1 Location of El Dorado Pilot Project within the Chesney Lease, El Dorado Field, Butler County, Kansas	3
2 Summary Flow Chart, Evaluation of Surfactant-Polymer Process Simulation, EOR	7
3 Direction of Data Gathering Flow from Micro- to Macro- to Megascale, versus Opposite Direction of Simulator Input Flow	12

TABLES

1 Outline, Data Requirements EOR Pilot Project Simulation	8
2 Data Requirement Categories EOR Pilot Project Simulation	9
3 Geologic Characterization, Category Descriptors	11
4 Reservoir Characterization, Category Descriptors	19
5 Process Characterization, Category Descriptors	26

ACKNOWLEDGEMENTS

GURC is responsible for the interpretation and opinions expressed herein, as contractor to Bartlesville Energy Technology Center (BETC) of the Department of Energy (DOE) for an independent study and assessment.

This study included subcontract work performed by Dr. Robert Berg, Texas A&M University, on the adequacy of available geologic data and its recommended use in geologic characterization of the reservoir, and by INTERCOMP Resource Development and Engineering, Inc., Houston, Texas, on data assessment and numerical simulation. Material from both subcontractors is contained in this report.

Following INTERCOMP's first report to GURC in May 1980, representatives of both organizations reviewed the assembled data and the simulation procedure. A final report with appendices was submitted to GURC in October 1980. The INTERCOMP reports are published separately as Appendix II and Appendix III.

Work done by GURC in this study has been under the supervision of Dr. Claude R. Hocott, Vice President for Energy Programs.

The cooperation and direct assistance of Cities Service Oil Company, operator of the El Dorado Project, is gratefully acknowledged. Principals in technical assistance were C. L. Coffman, Project Manager; Lyle Baie, J. Vairogs, R. Tillman, D. Jordan, and J. Fanchi. Any misinterpretation or misstatement of El Dorado data lies with GURC and not Cities Service.

ABSTRACT

The results of computer simulation of the El Dorado surfactant-polymer EOR pilot project, Butler County, Kansas indicated that conventional data from the project and other data in the public domain were not adequate for geologic, reservoir and process characterizations in a complex numerical simulation.

As used by GURC in geologic characterization, and by INTERCOMP in process characterization and input into the CFTE simulator, the collective body of field and chemical data and related assumptions necessary for simulator input was not sufficient to predict how the chemical flood would behave in the Admire 650-foot sandstone reservoir.

Based upon this study, a comprehensive body of data requirements for EOR simulation is defined in detail. Geologic characterization includes descriptors for rock, interwell and intrasystem correlations; reservoir characterization includes descriptors for fluid/rock, production, and flow rate properties; process characterization includes descriptors for chemical properties, interactions and functions.

Reservoir heterogeneity is a principal problem in EOR simulation. It can be overcome within reasonable economic limits by successive orders of descriptors from:

- o microscale (rock), achieved through borehole and core analyses, to
- o macroscale (interwell), achieved through multiple borehole correlations, to
- o megascale (intrasystem), achieved through extrapolation of rock and correlative well data into a generic depositional model that contains a description of internal mass properties within a given external morphology.

A flow chart for surfactant-polymer process simulation is included as Appendix I. Appendices II and III are INTERCOMP reports to GURC describing the CFTE simulator program used in this study.

1.0 INTRODUCTION

1.1 Purpose

An objective of the cooperative venture (joint-funded) EOR program established by the U.S. Bureau of Mines and subsequently administered by ERDA and DOE was to bring into the public domain sufficient information concerning given EOR processes that technology transfer could take place between companies or operators. Data on a given project could be used, with proper evaluation, to assess the technical and economic feasibility of initiating a similar EOR operation in a different section of the same field or in another field.

The method often used to analyzing and interpreting data generated from pilot projects is numerical simulation; therefore, the sufficiency of available data from a given project for numerical simulation of that project is a fundamental issue.

In 1978, GURC proposed to DOE to conduct a study involving the analysis by computer simulation of data generated in a typical demonstration project sponsored by DOE. The contract was awarded in September 1978. On June 1, 1979, INTERCOMP Resource Development and Engineering, Inc., was retained as a consultant to perform the computer simulation, using a proprietary finite-difference-based numerical reservoir simulator for predicting micellar/polymer flood performance.

The purpose of the study was to evaluate the adequacy of data placed in the public domain by a specified DOE cost-shared project. A secondary purpose, specified by DOE, was to establish guidelines for data requirements. Subsequently, with a lot more experience and a few more data, GURC and DOE reversed the emphasis in order to focus upon data requirements, with analysis of the pilot project as secondary.

1.2 Subject of Study

The Cities Service Company/DOE cost-shared El Dorado Micellar/Polymer Demonstration Project was specified as the subject of the study. Although the chemical flood project had been initiated about one-half year earlier, it became a cooperative venture by contract in June 1974. It was chosen for the following reasons, in addition to being a DOE-sponsored project:

- o chemical flooding was expected to have a large potential for enhanced oil recovery;
- o the project was sufficiently old to provide a considerable amount of field history;

- o a large quantity of data concerning the project had been placed in the public domain by the operator, through BETC and SPE publications; and
- o the operator is a GURC affiliate, enabling use of established lines of communication.

The El Dorado field in Butler County, southern Kansas, produced from several reservoirs, one of which was the Admire 650-foot sandstone. Primary and secondary recovery techniques had produced about 36.5 million barrels of oil from the 650-foot sand. An estimated 71.5 million barrels remained in place when the waterflood was abandoned in 1971. Because the 650-foot sand reservoir had been abandoned, any oil that was recovered by chemical flood would be truly tertiary oil. Surfactant-polymer flooding was selected by the operator to recover a portion of the remaining oil. Prior to field-wide implementation of the chemical process, a pilot test was undertaken to assess its economic and technical feasibilities.

Figure 1 shows the plan of the El Dorado pilot project. In the southern half, the Hegberg lease, a Union Oil Company soluble-oil process was being used. In the northern half, the Chesney lease, a high-water-content process had been implemented. The DOE joint-venture project was to provide a comparison between the two processes at the conclusion of the project. The Chesney lease and its associated process were chosen for the GURC/INTERCOMP study.

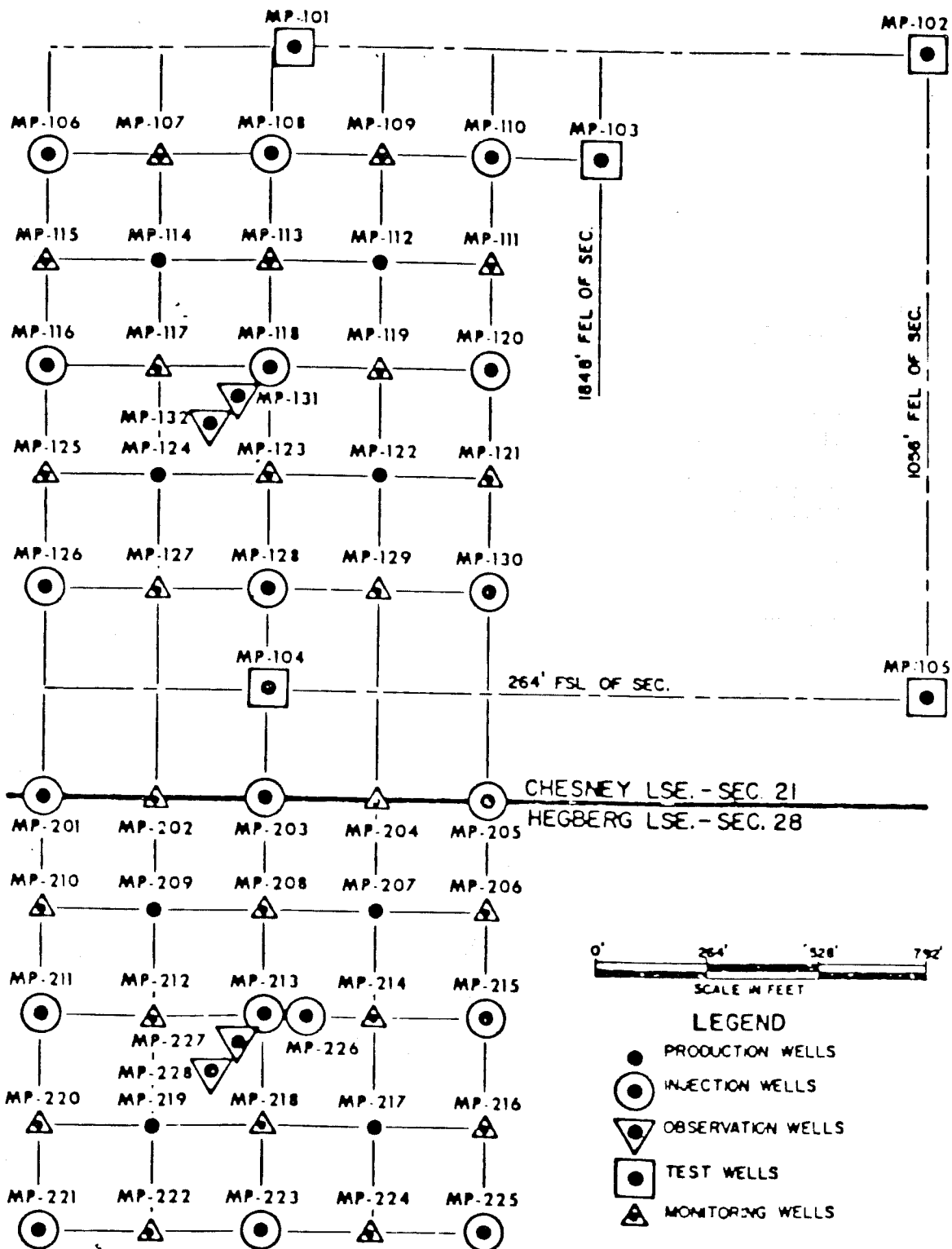
The high-water-content process used in the Chesney lease consisted of two low-salinity preflushes, followed by the surfactant slug, a tapered polymer slug, and by drive water.

1.3 Simulation Strategy

As outlined by GURC for the study, simulation of reservoir behavior with a numerical simulator is based upon a process of data assembly with iterative refinement. A geologic model is developed to describe the reservoir morphology, lithology and continuity. These concepts are expressed numerically as input into the simulator to constitute a reservoir model within which various processes can be carried out. Tables of physico-chemical data are prepared with respect to each process that is to be simulated. These data tables correspond to the needs of a physical-chemical description of the process which is already built into the computer program. As expressed mathematically, this is referred to as the process model.

Based upon these models, the simulator is used to generate a prediction of reservoir behavior. If sufficient field history has been generated, the predicted behavior can be compared to the actual field behavior. As is often the case, corrections are made to either or both of the models in order to achieve a history match.

When a history match is obtained, estimates of future reservoir performance are made for the particular reservoir and process whose histories have been matched.



U.S. GOVERNMENT PRINTING OFFICE 1976-149 362/11

Figure 1. Location of El Dorado Pilot Project within the Chesney Lease, El Dorado Field, Butler County, Kansas

2.0 SIMULATION PROBLEMS IN EOR CHEMICAL PROCESSES

A number of problems exist in numerical simulation of EOR chemical processes as a result of technical or economic limitations, such as:

- a. changes in ratios of capillary: viscous:gravitational forces which have effects other than mobilization of oil;
- b. effects of pore structure, which govern hysteresis in capillary pressure and relative permeability, and strongly affect oil and chemical entrapment;
- c. effects of interfacial forces, i.e., ratio of viscous to capillary forces, such that, for example, nearly complete oil recovery by EOR requires an increase by a factor of 10^4 or more in the capillary number;
- d. effects of wettability, which impact the response of residual oil to the chemical slug and the oil displacement efficiency of the process;
- e. collection and analysis of waterflood history prior to EOR pilot design, whereby through documentation of input/output data throughout a sufficiently fine grid, fluid flow zones are delineated and numerically summarized even though without generic descriptions;
- f. distribution and measurement of oil that is
 - o outside the fractional volume of a pattern swept by injected fluid (sweep efficiency),
 - o by-passed within the swept volume by lack of contact with injected fluid (contact factor), or
 - o remains as residual oil from the original oil saturation now displaced from rock pores by injected fluid (displacement efficiency);no simple way exists to determine where the remaining oil is located, but S_{or} is an essential key to both the technical and economic processes of EOR.
- g. the role of capillary pressure in EOR as in secondary waterflood where a prevalence of micro- and macro-heterogeneities has the same effect upon oil-water capillary pressure as does simpler, better-known stratifications;
- h. the role of authigenic and allogenic clay mineral assemblages in surfactant retention, and the frequent failure of core floods and core-flood simulation to predict either the presence or the adverse impact of clay minerals.

The major simulation problem, however, is reservoir heterogeneity, or non-uniform distribution of physical and chemical properties that impact fluid flow and the behavior and performance of injected chemicals. This problem results from both technical and economic limitations upon detailed reservoir description and its input into simulation programs.

The fundamental problem of heterogeneous reservoir rocks is the inability of the reservoir engineer and simulator to predict kind, magnitude and probable location of the non-uniformities within the reservoir system. The heterogeneities divert fluid flow through the reservoir to reduce sweep efficiency, prevent hydrocarbons from being contacted and displaced by injected liquids and contribute to breakdown of injected chemicals. They create errors in the numerical simulation which cannot be overcome within economical limits by adjusted black oil simulator test runs, adjusted process characterization, or adjusted core flood history matches. In the field, they generally complicate the EOR process to the point of economic failure.

Heterogeneity is the largest and least understood factor in EOR simulation and the leading cause of failure of EOR pilots to perform as predicted and models to match pilot performance.

In the words of Parke A. Dickey concerning geological limitations on enhanced recovery methods, "There are certain limitations to enhanced recovery methods resulting from the geology of the reservoir. These have not always been taken into account; if they had been, many disastrous failures could have been avoided. The greatest cause of trouble in either secondary or enhanced recovery methods is heterogeneity in the reservoir."¹

GURC does not maintain that the foregoing problems in EOR simulation are solved by better characterization. We do, however, believe that many simulation problems and failures can be eliminated by better characterization input into computer programs adequate to handle better data.

3.0 SIMULATION FLOW CHART FOR SURFACTANT-POLYMER PROCESS

In order to maintain an overview of the El Dorado field, Chesney lease, simulation which is uniform throughout the diversity of data sources and simulator input-output, GURC developed a relatively simple simulation flow chart for the surfactant-polymer process. This chart is Appendix I.

A skeletal summary chart of Appendix I is shown in Figure 2; however, this figure does not contain a number of tasks that are essential in the simulation procedure, as shown in Appendix I.

The flow chart for evaluation of surfactant-polymer process simulation of EOR is constructed in PERT chart language. Each box within the network of flowlines represents an accomplished task or milestone and the flowlines represent work being done to accomplish the milestones. The chart is not time-scaled.

The simulation process, as portrayed on the flow chart, consists of four phases:

- 1.0 collection, analysis, conversion of data from field and laboratory; construction and refinement of a reservoir model,
- 2.0 completion of process simulation,
- 3.0 history match comparison,
- 4.0 generation of conclusions.

Each phase excepting the last (4.0) includes one or more milestones of completed tasks numbered successively in the sequence in which they are accomplished, some with feed-back loops for reiterative adjustment of data input/conversion.

The first phase (1.0) is by far the most complex, variable and site-specific with respect to successful simulation by reason of the old adage: garbage in, garbage out.

Milestones within phase 1.0 of the flow chart are coded in two more or less parallel series: A for field data and geologic characterization, and B for laboratory data and process characterization. The A series occupies the upper portion of the chart; the B series, the lower portion.

The GURC flow chart for evaluation of surfactant-polymer process simulation contains within one milestone, A 1.4.2 "Tentative Geologic Characterization", a multitude of conclusions, interpretations and compilations that profoundly affect the outcome of the simulation but are not set forth and generally not used in present state-of-the-art in the detail shown in process characterization.

The relatively thin treatment of geologic characterization in the flow chart is commensurate with common industrial practice. It is portrayed in this manner to establish a comparison of "what" was developed with "how" it was developed.

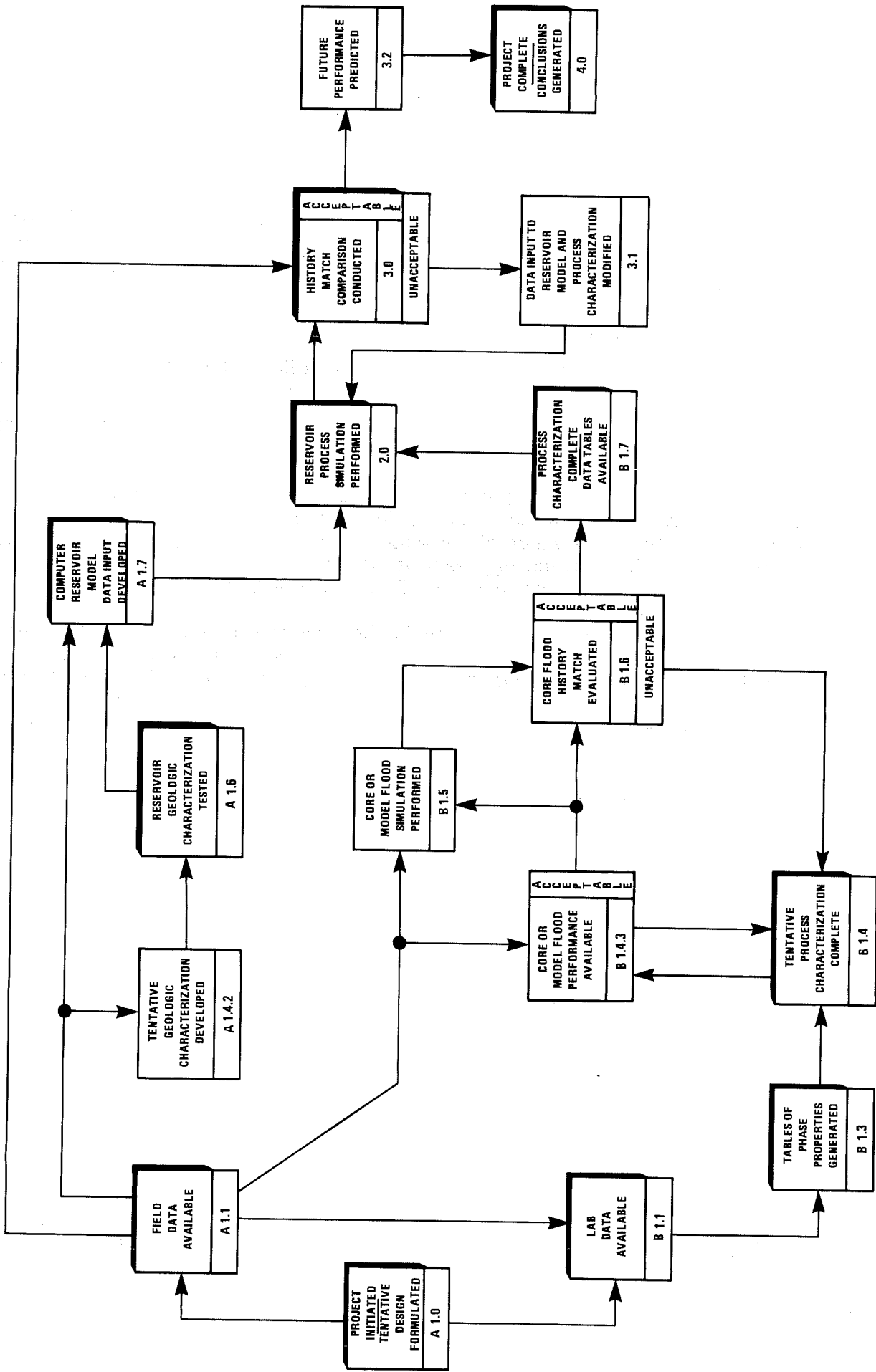


Figure 2. Summary Flow Chart, Evaluation of Surfactant-Polymer Process Simulation, EOR

4.0 DATA REQUIREMENTS

4.1 Introduction

The customary practice in numerical simulation programs of an EOR chemical pilot project emphasizes process characterization in detail commensurate with the great amount known about chemical processes, and feedback loops to fine-tune process characterization through:

- o core flood performance;
- o several or more sensitivity runs to adjust phase behavior, plug size, residual oil, etc; and
- o history match parameters such as core flood, field data, and field samples of injected chemicals.

EOR simulation at this point in time employs more understanding of chemical process characterization than of geologic characterization of the reservoir rock/fluid system into which the chemicals are injected. Other major issues in applications of EOR technology such as chemicals and economic evaluations, are described in GURC reports under J. R. Crump² and E. L. Secrest³.

To accompany the process-specific flow chart and reduce the imbalance of geologic versus process characterization, GURC has defined a body of descriptors, or data sets, necessary in varying degrees to characterize a chemical EOR pilot project (Table 1). The objective is to provide characterizations of the rock/fluid systems, and behavior of injected chemicals sufficient to eliminate most common simulation failures and reduce what cannot be eliminated.

TABLE 1

OUTLINE, DATA REQUIREMENTS EOR PILOT PROJECT SIMULATION

CHARACTERIZATION

CATEGORY

DESCRIPTOR*

SOURCE

OUTPUT*

SIMULATOR INPUT*

* Keyed to Appendix I, "Process Specific Flow Chart, Surfactant-Polymer Process Simulation", as appropriate.

As shown in Table 2, the GURC data requirements for EOR pilot project simulation, process-specific to surfactant-polymer, are classified into three characterizations (Geologic, Reservoir, Process), each with three categories of data in which Process Characterization also includes coreflood performance.

TABLE 2
DATA REQUIREMENT CATEGORIES
EOR PILOT PROJECT SIMULATION

<u>Characterization</u>	<u>Category</u>
Geologic	Rock
	Interwell
	Intrasystem
Reservoir	Fluid/Rock System
	Production
	Flow Rate
Process	Properties
	Interactions
	Functions
	Core Flood Performance

For each category, several or more Descriptors are defined, together with:

- o usual sources from which descriptor data can be derived,
- o output form in which the data are expressed, and
- o simulator input form in which the data are used.

In this report, Descriptors, Outputs, and Simulator Inputs are cross-referenced to Appendix I, the flow chart, by alpha-numeric notation.

4.2 Geologic Characterization

The principal objective of geologic characterization is to determine the size and distribution of grid blocks necessary for optimum portrayal of the reservoir system. Many geologic descriptors necessary for horizontal and vertical grid block definition do not go directly into the simulator but are no less important to the simulation.

As heterogeneity increases, grid block density must increase in order that the "average" values calculated in each grid block for simulator input indicate the rates and magnitudes of variation throughout the system.

The categories of data and their descriptors for geologic characterization of reservoir are listed in Table 3. The three categories are successive orders of scale from:

- o microscale characterization achieved through borehole and core analyses (Rock descriptor), to
- o macroscale characterization achieved through multiple bore-hole correlations (Interwell descriptor), to
- o megascale characterization achieved through extrapolation of rock and correlative well data into a generic depositional model of the reservoir which contains an orderly qualitative description of internal mass properties within a given external morphology (Intrasystem descriptor).

Quantification of descriptive data is a basic objective of well log and core analyses, and commences in the Rock descriptors. Quantification is extended laterally by means of borehole correlations and 3-D mapping of qualitative and quantitative data in and between bore holes. In-fill drilling certainly should be considered at this phase.

Extension of rock and borehole descriptive qualitative data to fill the network between well control and to extend the description beyond well control is an orderly extrapolation within the known qualitative limits of the rock unit, i.e., the appropriate generic depositional model.

In-fill drilling can be used to upgrade and/or verify intrasystem extrapolation of rock and wellbore correlations; conversely, intrasystem extrapolation can be used to plan infill drilling for production wells within heterogeneous oil entrapments and unflushed zones.

Similarly, rock and borehole quantification of qualitative description can be extrapolated between and beyond immediate well control within the known depositional model with accuracy sufficient to upgrade existing simulation techniques and to provide data that customarily are not used.

As illustrated in Figure 3, the description and accumulation of reservoir rock data progresses from (1) microscale rock measurements, including individual well logs and microscale heterogeneities in cores, to (2) macroscale well-to-well reservoir measurement, to (3) megascale extrapolation of cumulative descriptions throughout the rock model of known internal qualitative properties and external morphology.

Conversely, the organization of geologic characterization of simulator input progresses in the opposite direction from the order and structure of the megascale or magnitude of non-uniformities, i.e., heterogeneities, of the system.

A highly relevant philosophical principle to the foregoing is that "how we think" is epistemology, and epistemology is subject to modeling in every case.

TABLE 3

GEOLOGIC CHARACTERIZATION, CATEGORY DESCRIPTORS

ROCK	INTERWELL	INTRASYSTEM
Mostly Scalar Properties	Mostly Vector Properties, Planar and Linear	Vector, Planar and Linear
1. Formation elevations	1. Texture, mass properties,	1. Generic depositional model
2. Formation morphology a. lithologic boundaries b. structural boundaries c. thickness	2. Mineralogy/chemical composition, distribution	2. Diagenetic overprint
3. Sedimentary structures, internal	3. Flow unconformities	
4. Mineralogy/chemical com- position	4. Flow layers/zonations	
5. Texture		
a. individual properties b. porosity c. permeability		

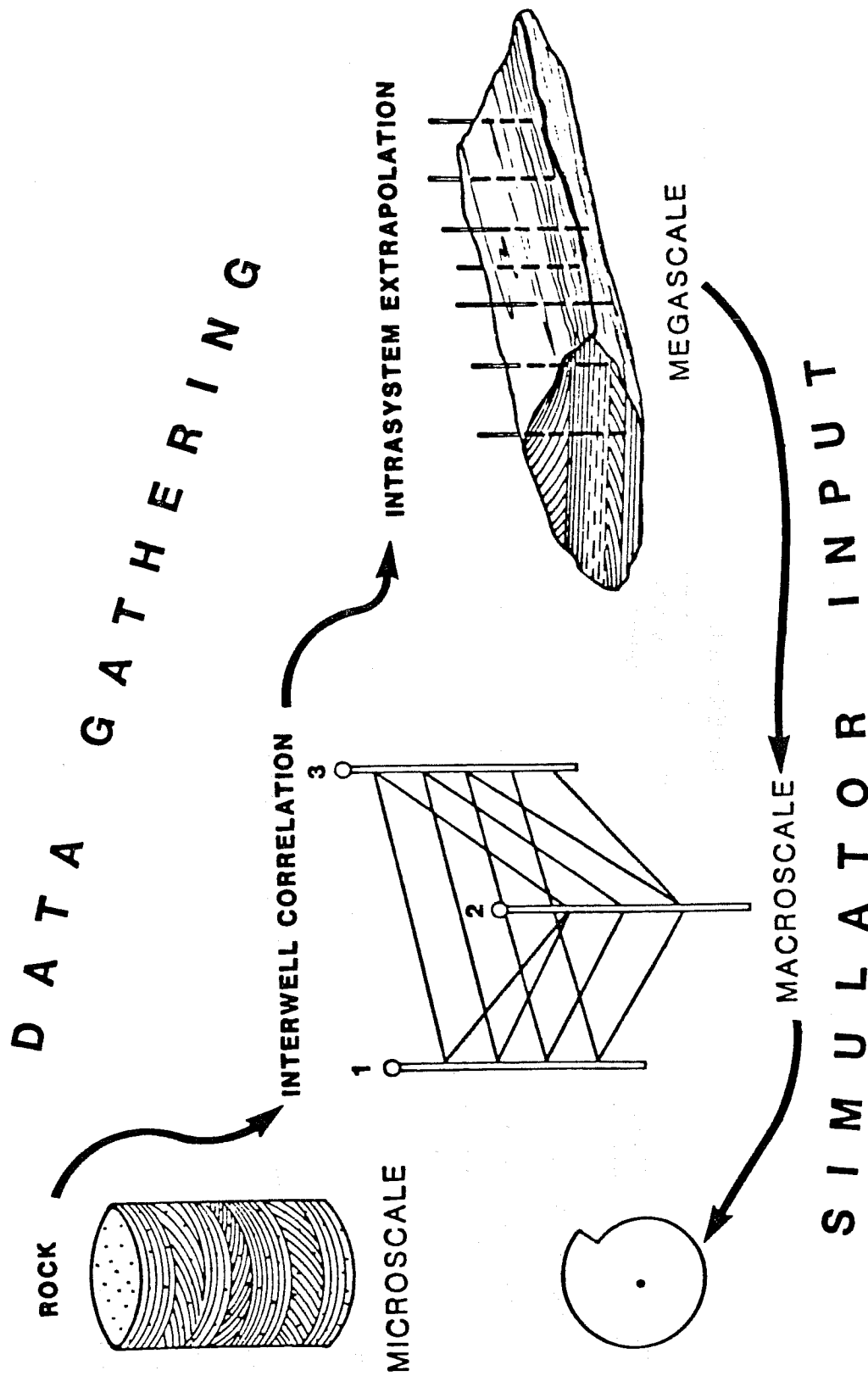


Figure 3. Direction of Data Gathering Flow from Micro- to Macro- to Megascale, Versus Opposite Direction of Simulator Input Flow.

4.2.1 Rock Descriptors

(1.) Descriptor:

FORMATION ELEVATIONS

Source:

Data from well logs, drilling records, seismic, sub-surface structural maps, single or multiple parameter.

Output:

Maps, cross-sections, tables

Simulator Input:

A 1.4.2 Geologic Characterization; as depths of centers of grid blocks, tables.

(2.) Descriptor:

FORMATION MORPHOLOGY

1. Lithologic boundaries
 - a. Location
 - b. Nature
 - (1) Conformable
 - (2) Unconformable
 - (3) Intergrade
 - (4) Intertongue
2. Structural boundaries/barriers
 - a. Fractures
 - b. Faults
3. Thickness
 - a. Gross
 - b. Net

Source:

Well log data, drilling records, seismic processing, cross-sections (structural, stratigraphic), subsurface structural maps, isopachous maps (gross interval, net lithotype interval, single and multiple parameter), generic depositional model.

Output:

Maps, cross-sections, tables; A 1.3 Depositional Environment.

Simulator Input:

A 1.4.2 Geologic Characterization

(3.) Descriptor:

SEDIMENTARY STRUCTURES, INTERNAL

1. Stratification
2. Lamination
3. Bedding
4. Unconformities

Source:	Well log data, seismic, cross-sections (structural, stratigraphic), subsurface structural maps, generic depositional model.
Output:	Maps, cross-sections; A 1.3 Depositional Environment
Simulator Input:	A 1.4.2 Geologic Characterization
(4.) Descriptor:	MINERALOGY/CHEMICAL COMPOSITION <ol style="list-style-type: none"> 1. Inert minerals 2. Diagenetic clays 3. Carbonates 4. Clay response to changes in: <ol style="list-style-type: none"> a. Salinity b. Ion concentration
Source:	Core analyses
Output:	Maps, cross-sections; A 1.4 Core Analyses, A 1.3 Depositional Environment
Simulator Input:	A 1.4.2 Geologic Characterization
(5.) Descriptor:	TEXTURE <ol style="list-style-type: none"> 1. Individual properties <ol style="list-style-type: none"> a. Particle size b. Particle shape c. Particle roundness d. Sorting e. Packing f. Fabric 2. Porosity 3. Permeability
Source:	Laboratory analyses, well log data, literature correlations; pressure test analyses (pressure build-up, fall-off); interference tests, regression analysis (case history).
Output:	Maps, cross-sections, lists; A 1.3 Depositional Environment
Simulator Input:	A 1.4.2 Geologic Characterization

* Muskat, Miller-Dyes-Hutchinson, Horner, type curve analysis.

4.2.2 Interwell Descriptors

(1.) Descriptor:

TEXTURE, MASS PROPERTIES

1. Porosity distribution
2. Pore size distribution
3. Permeability distribution
 - a. Relative permeability
 - b. Oil-water capillary pressure
4. Fabric
5. Particle surface area

Source:

Reference Rock Texture; correlation between boreholes, tracer tests, single and multiple parameter cross-sections and subsurface maps, literature correlation, generic depositional models.

Output:

Maps, cross-sections, tables; A 1.3 Depositional Environment; quantification of 3-D rock descriptors and characterizations.

Simulator Input:

Development of asymmetrical or symmetrical grids showing distribution of specified rock properties for individual sectors of reservoir represented by each grid, and the heterogeneous or homogeneous distribution of those properties throughout the layers of reservoir covered by the grids. A 1.4.2 Geologic Characterization.

(2.) Descriptor:

MINERALOGY/CHEMICAL COMPOSITION AND DISTRIBUTION

1. Inert minerals
2. Diagenetic clays
3. Carbonates
4. Clay response to changes in:
 - a. Salinity
 - b. Ion concentration

Source:

Core analyses, correlation between boreholes, single and multiple parameter cross-sections and subsurface maps, literature correlation, generic depositional models.

Output:

Maps, cross-sections, tables; A 1.3 Depositional Model. Quantification of 3-D rock descriptors and characterizations.

<p>Simulator Input:</p>	<p>Development of asymmetrical or symmetrical grids showing distribution of specified rock properties for individual sectors of reservoir represented by each grid, and the heterogeneous or homogeneous distribution of those properties throughout the layers of reservoir covered by the grids. A 1.4.2 Geological Characterization.</p>
<p>(3.) Descriptor:</p>	<p>FLOW UNCONFORMITIES</p>
<p>Source:</p>	<p>Pressure test analyses, tracer tests, secondary recovery waterflood histories, subsurface geologic correlations between boreholes (stratigraphic cross-sections); general depositional models in conjunction with high-resolution reflection seismics, vertical seismic profiling, cross-borehole seismic.</p>
<p>Output:</p>	<p>Maps, cross-sections, tables; A 1.3 Depositional Model. Recognition of number of effective flow layers necessary to be portrayed by asymmetrical grids and 1-D reservoir models.</p>
<p>Simulator Input:</p>	<p>Development of asymmetrical or symmetrical grids showing distribution of specified rock properties for individual sectors of reservoir represented by each grid, and the heterogeneous or homogeneous distribution of those properties throughout the layers of reservoir covered by the grids. A 1.4.2 Geologic Characterization.</p>
<p>(4.) Descriptor:</p>	<p>FLOW LAYERS/ZONATIONS</p>
<p>Source:</p>	<p>Reference GEOLOGIC, INTERWELL CORRELATION, Flow Unconformities; electromagnetic surveys (contoured source audio magneto-telluric CSAMT, time domain electromagnetic TDEM).</p>
<p>Output:</p>	<p>Maps, cross-sections, tables; A 1.3 Depositional Model. Definition of number of flow layers necessary to be characterized by asymmetrical grids and 1-D reservoir models.</p>
<p>Simulator Input:</p>	<p>Development of asymmetrical or symmetrical grids showing distribution of specified rock properties for individual sectors of reservoir represented by each grid, and the heterogeneous or homogeneous distribution</p>

of those properties throughout the layers of reservoir covered by the grids. A 1.4.2 Geologic Characterization.

4.2.3 Intrasystem Descriptors

(1.) Descriptor:

GENERIC DEPOSITION MODEL

1. Morphology
2. Heterogeneities
 - a. Macro-
 - b. Micro-
 - c. Physical
 - d. Chemical
3. Relative sedimentary structures
 - a. Inorganic
 - b. Organic
4. Relative textures (qualitative)
 - a. Particle size distribution, lateral and vertical
 - b. Mineralogy distribution, lateral and vertical
 - c. Permeability distribution, lateral and vertical
5. Fabric (qualitative)
6. Flow unconformities and zonations

Source:

Literature, public and private

Output:

Maps, cross-sections, tables; A 1.3 Depositional Environment. Extrapolation of quantitative characterization.

Simulator Input:

Completion of asymmetrical grids for heterogeneous reservoir flow layers.

(2.) Descriptor:

DIAGENETIC OVERPRINT

1. Textural
 - a. Secondary intergranular porosity
 - b. Secondary permeability
 - c. Pore throat geometry
 - d. Grain surface area
2. Authigenic mineralogy
clay mineral assemblages
3. Relative distribution of diagenetic changes, lateral and vertical

Source:

Laboratory analyses (electron micrographics, mercury injection and photomicrographs,

etc.); interwell correlations by single and multiple parameter cross-sections and sub-surface maps; extrapolation through generic depositional model.

Output: Completion of asymmetrical grids for heterogeneous reservoir flow layers.

4.3 Reservoir Characterization

The categories of data and their descriptors for reservoir characterization for EOR surfactant-polymer process simulation are listed in Table 4. The three categories progress from numerical descriptions of the fluid/rock system, to basic production history, to dynamics of wellbore/reservoir interface. Material presented here is selected principally from review of EOR pilot project reports from the U.S. Department of Energy and adapted in descriptive form for standardization from Craft and Hawkins⁴, Crichlow⁵, and Monicard⁶.

4.3.1 Fluid/Rock Descriptors

- | | |
|------------------|--|
| (1.) Descriptor: | FLUID BOUNDARIES |
| Source: | Seismic data, dry holes defining perimeter, core analyses, well log data, reservoir production data. |
| Output: | <ol style="list-style-type: none">1. Contour maps of:<ol style="list-style-type: none">a. depth of upper confining surfaceb. formation thickness (isopach)c. porosity times thickness (h)d. permeability times thickness (kh), ande. oil saturation (S_o).<p>Gas-oil and water-oil contact contour lines, if existent, are usually shown on maps of types <u>a</u> and <u>b</u>. A water saturation map (<u>e</u>) may also be provided.</p>2. Cross-section maps of the oil-producing formation. These are usually drawn through a series of wells lying approximately along a given compass direction, and bear the electric logs in a vertical direction at the well locations. Log indications of low porosity and permeability sublayers which form the upper and lower boundaries of producing layers are connected between wells, thus showing variations in thickness or even of discontinuities of layers. From their appearance, these are often called |

TABLE 4

RESERVOIR CHARACTERIZATION, CATEGORY DESCRIPTORS

Fluid/Rock System	Production	Flow Rate
1. Fluid boundaries	1. Time-rate injection history	1. Flow behavior at well-bore/reservoir
2. Fluid saturations S_{oi} , S_{or} , S_w	2. Time-rate production	
3. Relative permeabilities	3. Time-rate pressure	
4. Salinity a. Formation water b. Injected water		
5. Pressure-dependent properties a. Formation volume factor b. Fluid viscosity c. Solution gas-oil ratio		
6. Capillary pressure		
7. Capillary desaturation		
8. Pressure-temperature effects a. Ion exchange b. Dissolution c. Precipitation d. Adsorption e. Wettability		
9. Cation exchange capacity		
10. Dispersion coefficient		
11. Electrical Conductivity		
12. Compressibility		

"fence diagrams". It is helpful if these are constructed in more than one compass direction.

Simulator Input: Based on the region to be simulated (a pilot area, a symmetry element of a well pattern, or an entire field, each with one or more layers), a grid is selected to divide the simulated reservoir volume into blocks, within which the fluid and rock properties will be taken as the same over the block volume. This grid is superposed on the maps described above, and average fluid and rock properties are read from the maps and entered into tables which identify the properties with grid coordinates. Tables include block dimensions, porosity, permeability, and other data. These tables are input to the simulation. (A 1.4.1, A 1.4.2, A 1.7)

(2.) Descriptor: FORMATION FLUID SATURATIONS

1. S_{oi}
2. S_{or}
3. S_w

Source: Core analyses, well log data, capillary pressure data, tracer tests.

Output: A map of oil saturation and a map of water saturation.

Simulator Input: A table of oil and water saturations for each grid block in the simulation model is used as input. Gas saturation is calculated by difference ($S_o + S_w + S_g = 1.0$). (Part of A 1.4.1, A 1.4.2, A 1.7)

(3.) Descriptor: RELATIVE PERMEABILITIES

1. gas-oil
2. oil-water
3. gas-water

Source: 1. laboratory measurements (steady state displacement, unsteady state displacement),
2. calculations from capillary pressure data, field data, published correlations.

Output:

Relative permeability curves for:

1. simultaneous flow of water and oil, and
2. simultaneous flow of gas and oil

as functions of water saturation (a) or of gas (b).

Simulator Input:

1. In most simulators of the "black oil" type, relative permeability curves as described above are simply converted into tables and input to the simulation. The simulator program contains a procedure for calculation of three-phase relative permeability when three phases are flowing simultaneously (e.g., Stone's method, JPT, Feb. 1970, p. 214).¹⁶
2. In the chemical flooding simulator used in the work described here, the oil-water relative permeabilities are converted into Corey-type equations which fit the curves reasonably well. The constants of these equations are input to the simulator and are modified by a function of the capillary numbers in each grid block and at each time step. See B 1.2.2 and B 1.2.3.

(4.) **Descriptor:**

SALINITY

1. formation water
2. injected water

Source:

Laboratory analyses

Output:

An equivalent salinity (NaCl equivalent of mixed ionic composition) value for in-place water and a value for injected fluids in each state of the process.

Simulator Input:

Single values of salinity for injected fluids are input as part of the injection well data (which also contain well pressure limitations, fluid rate controls and type of fluid, and flow rate-determining data such as permeability and thickness of layers), for given time periods during which each fluid in the process sequence is injected, or for given total quantities of each fluid. (Part of A 1.2.3 and A 1.7)

- (5.) Descriptor: PRESSURE-DEPENDENT (PVT) PROPERTIES
1. formation volume factor (B_o FVF)
 2. fluid viscosity
 3. solution gas-oil ratio R_s GOR
- Source:
1. laboratory analyses
 2. estimation from empirical correlations based upon available data (e.g., gravity of tank oil, specific gravity of produced gas, initial producing gas-oil ratio, viscosity of tank oil, reservoir temperature, initial reservoir pressure) when laboratory data not available on reservoir samples.
- Output: Curves of B_o , R_s , and μ versus pressure (A 1.2.2).
- Simulator Input: The curves are converted into a table with pressure as the argument (independent variable) and are input directly in this form either into a "black oil" simulator (A 1.5) or a chemical flood simulator (A 1.7, AB 1.8).
- (6.) Descriptor: CAPILLARY PRESSURE
- Source: Laboratory data
- Output: Curves of:
1. gas-oil capillary pressure versus gas saturation
 2. oil-water capillary pressure versus water saturation
- Simulator Input: These are converted to tables and are input directly to "black oil" type simulators. The chemical flooding simulator does not use these data. In practically all cases where a chemical flooding simulator will be used, no gas phase will be present. The relatively small capillary pressure difference existing under chemical flooding conditions are neglected and the pressures in all liquid phases are assumed equal.
- (7.) Descriptor: CAPILLARY DESATURATION
- Source: Laboratory analyses

- Output: A curve of residual oil saturation (S_{orw}) and of connate water saturation (S_{wc}) versus capillary number $N_c (= u \mu / \sigma)$.
- Simulator Input: Tables are calculated of S_{wc} , S_{orw} , and of the constants of the relative permeability equations for oleic phase, aqueous phase, and for a micellar third phase (see Appendix D of INTERCOMP's report), for a series of values of N_c . In the simulations, values are interpolated for a given value of N_c in each grid block and at each time step (B 1.2.3, AB 1.8).
- (8.) Descriptor: PRESSURE-TEMPERATURE EFFECTS
1. ion exchange, cations and anions
 2. dissolution
 3. precipitation
 4. adsorption
 5. wettability
- Source: Laboratory measurements, generally at reservoir temperature and at atmospheric pressure.
- Simulator Input: These data form part of the process model (B 1.1.1, B 1.1.2, B 1.4.3.1, B 1.4.3.2, B 1.1.2, B 1.2.2).
- (9.) Descriptor: CATION EXCHANGE CAPACITY
- Source: Laboratory analysis, either by displacement tests or batch tests on disaggregated rock samples.
- Output: An average value
- Simulator Input: Part of process model data (B 1.1.1, B 1.2.1), input as a single value.
- (10.) Descriptor: DISPERSION COEFFICIENT
- Source: Field tracer tests give the values generally used. There is both a longitudinal dispersion coefficient, K_L , which can be determined from the curve of tracer concentration versus through-put by use of a mathematical equation based on one-dimensional flow, and a transverse dispersion coefficient K_t , which is generally estimated from the longitudinal

coefficient and other considerations (see Perkins and Johnston, SPE Journal, March 1963, p. 70).

	Output:	Single values of $\alpha_L = K_L/u$ and $\alpha_t = K_t/u$, since it is found that K_L and K_t are generally linear functions of the flow velocity u over the range of flow velocities of interest. Thus, α_L and α_t are approximately constant in a formulation of constant properties.
	Simulator Input:	A value of α_L and α_t (A 1.2.3, A 1.4.2).
(11.)	Descriptor:	ELECTRICAL CONDUCTIVITY
	Source:	Laboratory measurements on core saturated with brine of known conductivity.
	Output:	A formation factor F , which is used in interpretation of electrical logs.
	Simulator Input:	Not used in simulations.
(12.)	Descriptor:	COMPRESSIBILITY
	Source:	Laboratory analysis
	Output:	Values of compressibility for oleic phase, aqueous phase, micellar third phase, and of the pore space of the rock ("rock" compressibility).
	Simulator Input:	The single values of these four compressibilities are input.

4.3.2 Production Descriptors

(1.)	Descriptor:	TIME-RATE HISTORIES, EACH WELL, FOR: 1. injection 2. production a. oil b. water c. gas 3. pressure
	Source:	Records on production rates, pressures, composition data, (A 1.1.1); injection rates, pressures, composition data (A 1.1.2); previous production data (A 1.1.4); completion information (A 1.1.3) derived from data plotted and smoothed to extrapolate well data through missing points.

Output: Tables

Simulator Input: A 1.6 Black Oil Simulator, A 1.2.4 Well Characterization; ultimately, AB 1.8 Final Process Design, and 3.0 History Match Comparison.

4.3.3 Flow Rate Descriptors

(1.) Descriptor: FLOW BEHAVIOR AT WELL BORE/ RESERVOIR INTERFACE INDICATING RATE SENSITIVITY TO:

1. gas-oil ratio (GOR)
2. bottom hole pressure (BHP)
3. simultaneous solution of reservoir flow equation and multi-phase flow in vertical pipe.

Source: Calculations from productivity index or injectivity index.

Output: Tables, A 1.1.5 Reservoir Engineering Data.

Simulator Input: Simulators generally do not calculate flow pressure drops down injector wells or out of producing wells. Instead, bottom-hole pressures and rates are input as data, or one is specified and the other calculated. Flow is divided among phases or components according to relative permeabilities at producers or as specified in input data for injectors. Flow coefficients (or k and h data by layers) must be input as part of well data (A 1.2.4).

4.4 Process Characterization

4.4.1 Introduction

The categories of data and their descriptors for process characterization of EOR surfactant-polymer process simulation are listed in Table 5. The list encompasses combinations of descriptors whose tables of interactions include characterization of individual chemical properties/behavior. The basic process question is not what the characterization is, but how it interacts with other properties.

Coreflood performance is included in process characterization because of its essential role in adjustment of process data to make the model at this point, fit at least an elementary facet of the reservoir real world.

TABLE 5

PROCESS CHARACTERIZATION, CATEGORY DESCRIPTORS

<u>Properties</u>	<u>Interactions</u>	<u>Functions</u>
1. Formation resistivity factor, cation exchange data	1. Oil-water relative permeability versus capillary number	1. Coreflood performance
2. Non-polymer component density and viscosity data	2. Interfacial tension data	
	3. Surfactant-polymer viscosity versus concentration and shear rate data	
	4. Salinity requirement diagram data	

4.4.2 Properties Descriptors

(1.) Descriptor: FORMATION RESISTIVITY FACTOR AND CATION EXCHANGE DATA B 1.1.1

Source: Laboratory

Output: Cation Exchange Capacity, mg Ca/g rock;
Cation Exchange Equilibrium Coefficient,

$$K = \frac{(Cr^+)^2}{(C^+)} \frac{(C^{++})}{(Cr^{++})}$$

Cr^+ = meq monovalent cations per ml of pore space. Cr^{++} = meq bivalent cations per ml of pore space. C^+ = meq monovalent cations per ml of aqueous phase. C^{++} = meq bivalent cations per ml of aqueous phase.

Simulator Input: Formation Resistivity Factor is not used. Cation Exchange Data are entered as two tables for both of which the arguments and (1) the concentration of monovalent cations in the aqueous phase in the rock pores meq/ml and (2) the concentration of bivalent cations in the aqueous phase meq/ml. The entries in the first table are the meq of monovalent ions present on the rock surface per ml of pore space, and the entries in the second table are meq of bivalent ions on the rock surface per ml of pore space. B 1.2.1.

(2.) Descriptor: NON-POLYMER COMPONENT DENSITY AND VISCOSITY DATA B 1.1.6.

Source: Laboratory

Output: Density and viscosity of oil and brine, blending value of surfactant density and viscosity (in absence of polymer) and blending value of equivalent salinity.

Simulator Input: Single values of density and viscosity for each component (oil, water, surfactant) which can be used to calculate values of density and viscosity of each of the three phases which may be present, prior to determining effect of polymer concentration and shear rate on viscosity of phases containing polymer.

4.4.3 Interaction Descriptors

(1.) Descriptors:

OIL-WATER RELATIVE PERMEABILITY
VERSUS CAPILLARY NUMBER B 1.1.2.

Source:

Laboratory

Output:

(1) oil and (2) water phase permeability curves versus water saturation (at high interfacial tension, 30-35 dynes/cm). (3) gas and (4) liquid relative permeability curves versus gas phase saturation. Capillary desaturation curves for (5) oil phase and for (6) water phase as a function of capillary number $N_c (=u \mu / \sigma)$.

Simulator Input:

Equations are used for the relative permeability of each phase of the form

$$k_{ro} = (k_{ro})_{S_{wc}} \left[\frac{(1 - S_{orw} - S_w)}{(1 - S_{row} - S_{wc})} \right]^n$$

The values of $(k_{ro})_{S_{wc}}$, S_{orw} , and n are obtained from one or the other of two dummy variables which are linear functions of the logarithm of the capillary number, N_c . One of these dummy variables is the height of the desaturation curve for wetting phase and the other is the height of the desaturation curve for non-wetting phase, each being a function of the capillary number and ranging from 0 to 1.0. The constants of the equations of these lines are input data.

(2.) Descriptor:

INTERFACIAL TENSION DATA B 1.1.3.

Source:

Laboratory

Output:

Interfacial tension versus surfactant concentration, salinity in aqueous phase, and bivalent cation concentration in aqueous phase, for each pair of phases present at equilibrium.

Simulator Input:

Two tables of interfacial tension, one for oil phase versus micellar phase, the other for micellar phase versus aqueous phase, each with arguments of surfactant concentration and salinity. The salinity argument is an equivalent salinity, made up of the monovalent cation concentration plus a factor

times the bivalent concentration. This factor is input as part of the input data. B 1.2.3.

(3.) Descriptor: SURFACTANT-POLYMER VISCOSITY VERSUS CONCENTRATION AND SHEAR RATE DATA B 1.1.4.

Source: Laboratory.

Output: Curves of viscosity versus shear rate for each of the three phases (oil, micellar, aqueous) versus surfactant concentration, polymer concentration, and equivalent salinity (factor for bivalent cations determined experimentally).

Simulator Input: Tables instead of curves. B 1.2.4.

(4.) Descriptor: SALINITY REQUIREMENT DIAGRAM DATA B 1.1.5.

Source: Laboratory

Output: Phase volumes versus equivalent salinity (basis interfacial tension equivalence factor for bivalent cation concentration) and versus surfactant concentration, starting with equal volumes of brine and oil phase prior to addition of surfactant polymer. (Co-surfactant treated as part of surfactant.)

Simulator Input: A series of tables, each table for a given equivalent salinity, giving pairs of tie-line binodal points, including the pair of points at the base of the binodal curves, and the plait point where both values are the same. B 1.2.5.

4.4.4 Function Descriptors

Descriptor: PROCESS PERFORMANCE AS INDICATED BY COREFLOOD PERFORMANCE

Source: Laboratory

Output: B 1.4.1 Coreflood Design
B 1.4.2 Coreflood
B 1.4.3 Coreflood Performance data

Simulator Input: B 1.4.3.1 Pore volume inaccessible to polymer, input data single value.

B 1.4.3.2 Surfactant and polymer adsorption tables at weight adsorbed per gram of rock versus surfactant concentration.

B 1.4.4 Tentative Process Characterization (all tables previously described under PROCESS).

5.0 ANALYSIS OF EL DORADO SIMULATION

5.1 Introduction

The objective of this section is to comment on the GURC/INTERCOMP simulation with respect to the GURC definition of data requirements (Sections 3.0 and 4.0). In addition, the commentary includes:

- o EOR simulation in general;
- o reference to supporting university and industrial research, case histories and methodologies;
- o GURC staff opinions.

The following Sections 5.2 through 5.4 present assessment of the availability of sufficient data in amount and quality for Geologic, Reservoir and Process characterization respectively, and the use of available data in conducting a numerical simulation program of the industry/DOE cost-shared El Dorado demonstration project by parties other than the project operator.

5.2 Geologic Characterization

GURC held responsibility for providing to INTERCOMP the geologic characterization data for input into the CFTE simulator.

The GURC geologic description referred to "deltaic origin" of the Admire 650-foot sand, containing cross-bedding and interbedded shales; also, a basal "clean" sand with permeabilities as high as 1500 md present in some wells and absent in others. Two "zones" are reported: upper with porosities of 23 to 26 percent, gross thickness 7 to 15 feet; lower with porosities 19 to 25 percent, gross thickness 6 to 13 feet.

A number of contour maps were made of data derived from well logs and Epilogs using a computer plotting program commercially available. Log data were also digitized. The initial GURC maps included net and gross pay thicknesses, net to gross pay ratios, net porosity and permeability, oil and water saturations, and transmissibility.

INTERCOMP furnished GURC a copy of the asymmetrical grid they drew on large-scale plots obtained from Cities Service. The grid enclosed a certain number of streamlines within parallel series of "stream tubes" and with a chosen number (20) of grid blocks marked off along each stream tube. The crossing lines approximated isopotential lines.

The stream-tube patterns were overlain on the various contour maps to obtain representative grid sector values within each stream tube for:

- o upper zone - net pay, porosity, permeability, net-to-gross ratio,
- o lower zone - net pay, porosity, permeability, net-to-gross ratio,

- o upper and lower zones - horizontal to vertical permeability ratios,
- o upper and lower zones - water saturation.

These values were also set into tables and forwarded to INTERCOMP in tabular format.

Subsequently, GURC obtained photographs of Admire 650-foot sand cores and additional pressure transient data that provided grounds for revised interpretation of the nature and distribution of the reservoir zones. As a result, a number of maps were redrawn and transmissibility values were recalculated. These revisions were, however, too late for INTERCOMP's input into the simulator.

The geologic investigation included a subcontract study by Dr. Robert R. Berg, Department of Geology, Texas A&M University, for geologic characterization of the Admire 650-foot sandstone reservoir in the El Dorado project.⁷

Dr. Berg's report stated: "Sedimentary structures determine the anisotropy of the reservoir sandstone to the flow of fluids. Composition and texture control porosity and permeability. Variations in composition and texture result in non-uniformity of fluid flow within the reservoir. Therefore, the main objective of geologic study is to determine the distribution of porosity and permeable zones between wells.

Porosity and permeability, in turn, control the distribution of oil saturation. Consequently, only by a study of the rock properties can reliable estimates be made of residual oil saturation between wells. The accurate determination of oil saturation is the basic problem in enhanced oil recovery, and no solution is possible unless the rock character is understood."

Dr. Berg first reported a composite of subenvironments of deposition based upon literature survey. In a supplementary report based upon examination of the core photographs not previously available, he concluded "that the entire section consists of a single, composite sequence of fluvial channel sandstones that were probably deposited in a low-sinuosity (braided) channel system."⁸

INTERCOMP reported to GURC with respect to its subcontract work in simulating the El Dorado Project.⁹ "The CFTE simulator provides a means to describe reservoir heterogeneity in considerable detail. This includes the distribution of permeability (horizontal and vertical) and porosity, areally and by layer, and net pay thickness by layer.

"Geologic data for the Admire (Chesney) sand were used by GURC to prepare a two-layered heterogeneous model of the reservoir element to be simulated.

"While the reservoir characterization was not one of INTERCOMP's tasks, we would like to comment that it is at least as important as the process characterization, if not more so, to the overall understanding and interpretation of a field test." (Italics provided by GURC.)

INTERCOMP further reported: "A generalized reservoir grid containing the four wells was generated from streamtube maps provided by Cities Service

Company. The map used was calculated using a homogeneous, isotropic reservoir description, average flow rates, and a unit mobility ratio between displaced and displacing fluids. The 5 x 20 reservoir grid...was created from flow and isopotential lines derived from the streamtube data....the flow paths at the top of the element are distorted because of poor production rates in the producer immediately above the element. The converging streamtubes at MP-124 accelerate the times of arrival of fluid fronts at the producing well, while grid effects only slightly influence the performance of the second observation well and do not disturb performance at MP-131.

"Despite these drawbacks and the fact that the asymmetric grid is not necessarily representative of the average pattern performance, it is without question the best grid possible to model the selected element. If average pattern performance is desired, then a representative one-eighth of a five-spot can be chosen which is homogeneous and symmetric. However, if a specific area of the reservoir is to be modeled, as was the case in this project, the most economical way to accomplish this is to generate an asymmetric grid which is parallel and perpendicular to the isopotential lines for this region.

"The geologic model imposed on the asymmetric grid was developed by GURC from log and core data. A two-layer model was described for the simulation element...This description shows the reservoir is of generally poorer quality in the vicinity of MP-132 and MP-123 (an inactive well south of MP-118). This two-layer description was used for cross-section simulations in the center streamtube of the asymmetric grid. For the areal simulations, a one-layer reservoir description was constructed from the two-layer model." (Italics provided by GURC.)

The GURC geologic description was based upon machine-plotted maps of log-derived parameters without modification for interpretive geological thinking.

The proposed two-layer geologic model was not compatible with observed behavior at one or more observation wells, and was acknowledged to be inadequate in reflecting reservoir heterogeneity. Only oil saturation and vertical communication between zones were altered for the simulations; no sensitivity runs with other adjustments to geologic parameters were performed in the geologic model (Section 4.0, Reference 8).

Asymmetrical streamtube patterns obtained from Cities Service were products of a simplified reservoir characterization. Cities Service reported in 1976: ¹⁰ "Four computer programs were developed to assist in the design of the field demonstration project. All of these programs assumed a consistent thickness, homogeneous reservoir with isotropic permeability. They also assume unit mobility between each injected slug and the fluids it displaces. Image wells may be used to simulate reservoir boundaries."

The Cities Service computer programs were applied, however, to a reservoir described in converse terms in the same paper "several project injection wells exhibited poor injectivity due to low permeability and low net thickness...large variations of permeability with location and direction that are indicated by both pressure transient analyses of old waterflood performance would be very detrimental..." and "...the reservoir is sandstone interbedded with shale. The net thicknesses vary upward to 30 feet, porosities vary upward to 30 percent and permeabilities vary between 50 and 1500 md...initial pattern selection work assumed a uniform thickness, homogeneous, isotropic reservoir and constant-rate wells..."

INTERCOMP simplified the geologic characterization of reservoir properties by combining into one layer the GURC two-layer descriptions. Sensitivity simulations made on phase behavior, preflush, slug size and residual oil saturation did not include reservoir geometries. In simulating field performance, no adjustments were made to relative permeabilities. History match parameters included optimal salinities of coreflood and field data, concerned with phase behavior, but not reservoir non-uniformities in lateral or vertical extent. A "black oil" reservoir simulation was not run for verification of reservoir characterization by history matching field performance or engineering data.

In review of the El Dorado simulation by INTERCOMP and GURC, one industrial peer review member reported¹¹, "We feel that the study contains deficiencies in the assumptions made, the appropriateness of the methods of modeling the process chemistry, and the conclusions reached on the basis of the study.

"The study predicts poor recovery due to trapping of type III microemulsions and subsequent lagging of the polymer bank by the surfactant. This lag is contrary to both laboratory and field experience. It is possible that these results are due to the use of a constant optimal salinity value (contrary to laboratory results, and recognized in the body of this report) and to the use of a relative permeability model that does not adequately represent the process.

"The study states that 'the effect of polymer viscosity reduction due to bacterial activity was not significant.' This conclusion is unwarranted unless the simulator explicitly takes into account viscous fingering. The body of the report states that the loss of polymer viscosity was modeled by injecting drive water without polymer. This method may account for loss of displacement efficiency due to fractional flow effects, but no evidence is given that viscous fingering is considered."

Further commentary is provided by an academic peer review member who said:¹² "...the use of only one or two layers in a simulation where vertical effects can be very important seems a bit too simple, even if the sand can be considered quasi-homogeneous (or randomly heterogeneous). In fact, I would have liked to have seen more 2-D runs both vertically and areally. The use of the streamlines...is, of course, approximate at best and does not really account for even drift properly, let alone areal heterogeneity.

"...The simulated and actual electrolytes for MP-132 are totally different. This is perhaps the most crucial issue in the report because of its implications with respect to oil recovery, etc. It is hard to imagine the simulator itself being that far off, so I assume the difference is due to a serious problem such as drift or geological aberration not accounted for and which literally demands attention and resolution. The simulator is telling us something here!"

All participants agreed that insufficient geological characterization data were available in the "public domain". Berg summarized the situation in his report to GURC:¹³ "...published reports do not contain sufficient information in order that geologic characterization of the reservoir sandstone may be made. The most important shortcoming of the published reports is the fact that detailed core descriptions of typical reservoir sections were not included. Furthermore, the results of petrographic analysis have not become part of the public record, and sampling for these analyses was inadequate for most of the cores."

5.3 Reservoir Characterization

5.3.1 Fluid/Rock Descriptors

(1.) Fluid Boundaries

The target for oil recovery processes in any given reservoir is determined by the volume enclosed by the boundaries of the reservoir (both vertical and areal) and by the concentration of oil within that volume. At an early stage in the development drilling of a given reservoir, the knowledge of boundaries is limited to estimates based on prior seismic work from which the shape of upper and lower confining surfaces can be determined, plus indications from the first well or first few wells as to the presence of a gas cap and/or a bottom water contact, and data from pressure transient tests which (if the reservoir is not connected to a gas cap or an aquifer) may indicate the total oil volume responding to the tests.

At a late stage of development drilling, the areal boundaries will have been fairly well defined by dry holes just beyond the perimeter of the field, and the vertical boundaries will have been rather accurately defined by core analyses and log data from a considerable number of wells, and by much more accurate volumetric determinations. It is important that cores be drilled in sufficient wells to sample all of the different rock facies present in the reservoir as a consequence of the various depositional processes which occurred when the reservoir rock was deposited. The examination of these cores by geologic and petrophysical methods performs two functions: (1) it identifies the depositional processes and locates where in the reservoir, both vertically and areally, each process was responsible for the rock which is present, and (2) it provides data on porosity and permeability and (less accurately) on saturations of oil, water, and gas; these data may be correlated with electric logs and neutron and gamma-ray logs in the same wells where the cores were obtained to make possible estimates of those quantities in other wells which were not cored but in which the logs have been run.

Identifying and locating rock deposited by recognized depositional processes makes it possible to estimate the likelihood of continuity or discontinuity of those given rock types or depositional features in the regions between wells where there is little or no direct information.

If it is likely that observed layers are continuous between wells, even though they vary in thickness, porosity, and permeability from well to well, then it is not unreasonable to draw contour maps of these quantities which fit the data at the wells. This makes it possible to overlay a grid map of the reservoir in computer simulations, and to read off average values of each quantity within each grid block, both areally and for each layer of such blocks representing the reservoir layers. Wherever there are discontinuities, these can be represented by introducing no-flow

boundaries between blocks on opposite sides of the discontinuity (either areally or vertically).

(2.) Formation Fluid Saturations

At the start of a reservoir simulation, it is necessary to specify the contents of each block in the three-dimensional grid of blocks representing the reservoir, as a saturation fraction (volume fraction based on pore volume) of gas phase, oil phase, and water phase. The data are obtained from core analyses and electric logs, plus initial production data (e.g., drillstem tests). Certain core tests, such as capillary pressure and relative permeability curve determinations, help to establish the minimum (connate) water saturation S_{wc} , the minimum oil saturation attainable by exhaustive waterflooding S_{orw} , and the minimum oil saturation attainable by exhaustive gas drive S_{org} .

At the beginning of oil recovery, the oil saturation in the oil column (below a gas cap, if present, and above bottom water, if present) is equal to $1 - S_{wc}$. However, if the reservoir simulation is to begin after some extent of primary recovery has taken place, dissolved gas may have come out of solution in the oil to form a free gas phase existent as tiny bubbles in the pores, surrounded by oil and water. At a gas phase saturation called the critical gas saturation, S_{gc} , the bubbles begin to connect between pores and travel as a separate phase to the production wells. The oil phase shrinks in volume as the dissolved gas evolves. In order to start a simulation at this point, it is necessary to know (or to estimate) the distribution of the free gas saturation over the three-dimensional grid representing the reservoir. Because of the difficulty of estimating this distribution, it is generally better to start simulation of primary recovery at the initial reservoir conditions.

For simulation of waterflooding (secondary recovery), it is possible to follow one of three alternative procedures: (1) first simulate primary oil recovery, starting from initial conditions, then start injection of water at selected wells and continue until the water cut increases (or oil production decreases) to an economic limit, (2) a waterflood may be started with the average free gas saturation present in every grid block, and continued until an economic limit is reached, (3) a waterflood may be started with the correct initial amount of stock tank oil in place but with the lower dissolved gas content expected to occur after the free gas phase is all either re-dissolved in the oil phase or is driven out of the production wells. The known primary oil production (as stock tank oil) is deducted from calculated waterflood production to obtain the predicted waterflood oil recovery, up to the economic limit.

In simulation of tertiary recovery, it is necessary either to simulate all of the previous processes, or to specify the distribution of oil and water saturations after waterflooding (a free gas phase is usually not present). It is possible by means of a single-well tracer test¹⁴ to determine the immobile oil saturation in the vicinity of a well. There are also logging methods and a pressure core barrel plus

core analysis method for determining the existing residual oil saturation at a well. There are also indirect methods¹⁵ which give only reservoir average oil saturations or regional oil saturations. Because of the difficulties of accurately determining or estimating the distribution of oil saturation at the economic limit (or later or earlier) in a water flood, it is not unusual to perform tertiary oil recovery simulations in which the residual oil saturation for exhaustive waterflooding, S_{orw} , is specified as the starting oil saturation in all of the grid blocks of the reservoir grid block model. This was done, for example, in the simulations performed by INTERCOMP on the El Dorado field. It is clear, however, that if the oil saturation actually present in the field is higher or lower than the assumed starting oil saturation in the simulation, the amount of oil present may be significantly different and the results of an effort to history match field performance may be affected.

(3.) Relative Permeabilities

In "black oil" simulators which can adequately simulate primary recovery and secondary recovery by waterflooding, it is necessary to be able to describe the simultaneous flow of gas and oil, gas and water, oil and water, or of gas plus oil plus water (three phases flowing simultaneously). The flow coefficients for each phase (k_{rg} , k_{ro} , k_{rw}) which are multiplied by the total permeability k of the rock to determine the permeability of the rock for each phase (k_g , k_o , k_w) are functions of the phase saturations.

Typically, three-phase relative permeability data (where all three phases are flowing simultaneously) will not be available for a given reservoir rock. There are few data in the literature, and most laboratories are not equipped to obtain such data. On the other hand, data are usually available or readily obtainable in laboratories on two-phase simultaneous flow. These data are usually for gas and oil and/or for oil and water. Oil is usually (but not always) the non-wetting phase with respect to rock grains in oil-water simultaneous flow. Gas phase is essentially always non-wetting with respect to both oil and water (though carbon dioxide at conditions where its density approaches that of crude oil may be an exception). When this is the case, the relative permeability to water phase is a function only of the water phase saturation, and the gas phase relative permeability is a function only of gas phase saturation. If oil phase is flowing simultaneously with both gas and water, its relative permeability is not a simple function of its own saturation. Various methods have been devised to calculate the oil phase relative permeability, of which the best known is Stone's method.¹⁶ (See also Dietrich¹⁷.) In most "black oil" simulators, water-oil and gas-oil relative permeability data are input as tables, and three-phase relative permeabilities are calculated from these data internally in the computer program.

In an enhanced oil recovery process simulator (miscible, chemical, or thermal), the calculation of relative permeabilities becomes more complex. Specifically, in the case of chemical flooding, a third liquid phase appears under some circumstances of equivalent

salinity and surfactant composition. Since the process is practically always applied after waterflooding, a gas phase is generally not present and so is not accounted for in most chemical flooding simulators. In general, no relative permeability data exist for the third liquid phase, but its relative permeability must be calculated within the simulator program.

Water-oil relative permeability curves obtained at very low capillary number ($N_c = \frac{k \nabla P}{\sigma}$) are used to generate all of the relative permeabilities calculated by the simulator. In the INTERCOMP simulator, the mathematical method devised by L. W. Lake, as described in Appendix D of the INTERCOMP El Dorado report, is used.

This method involves fitting both the oil and water phase relative permeability curves with a single-term power function:

$$k_{ro} = (k_{ro})_{S_{wc}} S$$

$$k_{rw} = (k_{rw})_{1-S_{orw}} (1-S)^p$$

$$S = (S_w - S_{wc}) / (1 - S_{orw} - S_{wc})$$

All three phases are present,

$$g = S_o (1 - S_w) / (S_o + S_w)$$

$$S_{mr} = S_{orw} + g(S_{wc} - S_{orw})$$

$$(k_{rm})_{1-S_{mr}} = (k_{ro})_{S_{wc}} + g [(k_{rw})_{1-S_{orw}} - (k_{ro})_{S_{wc}}]$$

$$r = n + g(p - n)$$

$$k_{rm} = (k_{rm})_{1-S_{mr}} [(1 - S_o - S_w - S_{mr}) / (1 - S_{orw} - S_{wc} - S_{mr})]^r$$

functions of the capillary numbers: $N_c (= u \mu / \sigma)$ the end-point relative permeabilities $(k_{ro})_{S_{wc}}$, $(k_{rw})_{1-S_{orw}}$, $(k_{rm})_{1-S_{mr}}$ and the exponents n , p , and r .

It is not known how accurate this method is although it has correct values at the limits and at low capillary numbers. Some method must be employed, because all of these relative

permeabilities, varying with N_c , must be calculated. The estimated oil recovery is a direct function of these calculations.

(4.) Salinity

The equivalent salinity (concentration of monovalent cation compounds plus a factor usually taken as 10 times the concentration of bivalent cation compounds) affects the process behavior of chemical flooding, caustic flooding, and polymer flooding oil recovery processes. Hence it is necessary to specify the equivalent salinity of the water phase present in a reservoir at the start of a simulation, as well as the equivalent salinity of each injected aqueous fluid. This enables the calculation of the equivalent salinity of the water phase in each grid block as the simulation proceeds. Standard methods of water analysis, applied to in-place water and to proposed aqueous fluids to be injected, provide the necessary values for input data to simulation.

(5.) Pressure-Dependent (PVT) Properties

Curves of the formation volume factor B_o , the solution gas ratio R_s , and the oil viscosity μ_o are measured in the laboratory on samples of reservoir crude oil obtained by re-combining separator gas and separator crude oil samples at a gas-oil ratio appropriate for the field, by well-known methods. These plus calculated curves of gas formation volume factor B_g and gas viscosity μ_g are generally input in tabular form with pressure as the argument (the variable with which the table is entered to find the other data mentioned, by interpolation), in "black oil" simulators. Water viscosity is usually input as a constant or with a single value at a reference pressure times a pressure coefficient:

$$\mu = \mu_{P_{ref}} [1 + C_\mu (P - P_{reference})]$$

In chemical flooding simulators, gas phase data are absent. The solution gas ratio and B_o are taken constant at the values following waterflooding. Viscosities are calculated for phases as a complex function of their compositions (including polymer).

(6.) Capillary Pressure

Gas-oil and water-oil capillary pressure curves are measured in the laboratory and are input as tables to "black oil" simulators. They are not used in INTERCOMP's chemical flooding simulator.

(7.) Capillary Desaturation

The residual oil saturation in the presence of water phase, and the minimum attainable aqueous phase saturation in the presence of oil phase, are found to start declining as the capillary number $N_c (= u \mu / \sigma)$ of about 10^{-4} , and reach values near zero at $N_c \approx 10^{-1}$. Since this change in the residual oil saturation is the purpose of chemical flooding, representing oil displaced, it is necessary to have either a standard curve applicable to all oils and rocks, if such a standard curve exists, or else to measure the curve experimentally for each

rock and crude oil. The only measurements of this curve which have been published are for Berea rock with several different oils¹⁸ and for a variety of water-wet rocks with refined oils¹⁹. The curves for carbonate rocks differ from those for sandstones in Abrams' work, but the curves for different sandstones are similar; however, for different rocks the midpoint value of the residual oil saturation is distributed over a range from about 2×10^{-4} to 2×10^{-3} . Thus, there does not appear to be a single standard curve, so it is necessary to measure several values on the curve for a given reservoir rock and crude oil in the laboratory. The data thus obtained are input in tabular form with N_c as the argument.

(8.) Pressure-Temperature Effects

The ion exchange capacity for monovalent versus bivalent cations for a given reservoir rock, and data on polymer and surfactant adsorption versus concentration and equivalent salinity of the aqueous phase, are obtained by published laboratory methods. The ion exchange capacity Q and the equilibrium coefficient K for such exchange are input as single average values for a given reservoir. The adsorption data for polymer and for surfactant are each input as a two-dimensional table with both concentration and equivalent salinity as the two arguments.

Other data such as dissolution or precipitation of rock components and rock wettability are not used directly in a chemical flooding simulator such as INTERCOMP's.

(9.) Cation Exchange Capacity

Reference Pressure-Temperature Effects, above.

(10.) Dispersion Coefficient

Reservoir simulators produce a spurious dispersion²⁰ due to the discretization of saturations (constant value over a given grid block, discontinuous changes between adjacent grid blocks, batchwise transfer of fluids between blocks at each time step). It is possible, however, to minimize such numerical dispersion by appropriate means²¹. It then becomes possible to incorporate a longitudinal dispersion coefficient K_L into reservoir simulation as a function of velocity u times a longitudinal mixing length α_L , $K_L = u \alpha_L$, and a transverse dispersion coefficient, $K_t = u \alpha_t$. These dispersion coefficients may then be used to calculate a concentration (saturation) gradient. This is done in INTERCOMP's chemical flooding simulator. It is described in a paper by Todd and Chase²². The subject of longitudinal and transverse dispersion is discussed by Perkins and Johnston²³.

(11.) Electrical Conductivity

For calibration of electrical logs, the formation factor $F = R_o/R_w$ (brine saturated rock resistivity divided by brine resistivity) is desired, together with the resistivity of in-place brine. The value of F is related to the porosity and the tortuosity of the rock pores by $F = \tau^2 / \phi$, where τ is the tortuosity and ϕ the porosity, and by the

empirical Archie relationship $F = 1/\phi^m$ and the Humble equation $F = 0.62/\phi^{1.5}$. When oil phase is also present, there is involved a saturation of water phase so that $R_t/R_o = 1/S_w^n$, where R_t is the resistivity of the partly oil-saturated, partly brine-saturated rock and R_o is the resistivity of the rock when $S_w = 1.0$. The ion exchange capacity of the clays within the rock structure also has a significant effect²⁴.

(12.) Compressibility

Compressibility is expressed as $c = (dV/dP)/V$. Values may be obtained by standard methods for the various phases which may be present (laboratory measurement for oil phase, obtained during PVT test, calculated for gas phase, known for water), and for the pore space of the rock (laboratory measurement using a fluid of known compressibility).

5.3.2 Production Descriptors

(1.) Time-rate histories, each well, for

1. injection
2. production
 - a. oil
 - b. water
 - c. gas
3. pressure

These historical data are important if the reservoir model derived from geological and petrophysical studies is to be verified through history matching with a "black oil" simulator. This is generally recommended. It will not only aid in improving the reservoir model but will give oil and water saturation distributions and the pressure distribution over the reservoir at the start of tertiary recovery operation.

This was not done in the case of El Dorado by INTERCOMP.

5.3.3 Flow Rate Descriptors

(1.) Flow behavior at well-bore-reservoir interface indicating rate sensitivity to

1. gas-oil ratio (GOR)
2. bottom-hole pressure (BHP)
3. simultaneous exhibition of reservoir flow equation and multi-phase flow in vertical pipe.

These data are of interest to the field engineer but are generally not used in simulations.

5.4 Process Characterization

5.4.1 Properties Descriptors

The following material is cross-referenced to Appendix I.

(1.) Formation Resistivity Factor and Cation Exchange Data B 1.1.1.

Discussion. The formation resistivity factor is measured in the laboratory on core samples from a given field in order to provide a calibration for electric logs runs on wells in the field. It is not used in calculation of process behavior and is not part of the input data for computer simulation.

The cation exchange data consist of two items: (a) the cation exchange capacity and (b) the cation exchange equilibrium coefficient.

(a) Cation Exchange Capacity

The cation exchange capacity of reservoir rocks is due in the case of sandstones to the presence of clay minerals which have ion-exchange properties. The existence of mobile ions in the clay minerals has the consequence that the electrical resistivity (or its reciprocal, conductance) is not a function only of the presence of electrically-conducting aqueous phase in the connected pores but also of the clay electrical properties. The sand grains are essentially non-conductive of electricity, but the clay minerals may contribute a significant degree of electrical conductivity; however, it is necessary that aqueous phase be present to transport counterions (negative ions) in the reverse direction to transport of the cations (with positive charges).

Based on the techniques developed in the soil science field²⁵, early techniques for determination of the ion-exchange capacity of rock formations involved grinding up the rock and measuring the ion-exchange capacity by converting the ion-exchange minerals to the Ba^{++} -saturated state and then electrometrically titrating the aqueous phase (distilled water of low conductivity) in contact with the ground-up sample with a solution of $MgSO_4$. The Mg^{++} would replace the Ba^{++} , forming $BaSO_4$ in the aqueous phase; the $BaSO_4$ is very insoluble and so the conductivity of the solution does not rise until all of the Ba^{++} has been replaced by Mg^{++} and an excess of the conductive $MgSO_4$ begins to appear in the aqueous phase. However, as pointed out by Grim²⁶, the apparent cation exchange capacity increases with the extent of grinding, hence it is apparent that grinding of core material beyond the degree required for grain disaggregation is inappropriate. Creation of ion-exchange sites by fracturing of mineral grains should be avoided.

Hill and Milburn²⁷ used chromatographic exchange of ammonium ion with other cations present in core samples to determine exchange capacity in displacement tests using ammonium acetate solution. Waxman and Smits²⁸ showed how the exchange capacity obtained by either method could be used in interpreting

formation rock conductivity (and thus the formation resistivity factor). Thomas²⁹ discusses an electrical "membrane" method of measuring the cation exchange capacity of cores.

In the 1970's it was realized that exchange of monovalent and bivalent cations between clays and solutions containing chemical flooding agents will affect the performance of these agents³⁰⁻³⁶. In most of the work reported, the cation exchange capacity was determined by the soil science titration method³⁷.

The data available from Cities Service Company on the ion-exchange capacity of El Dorado field, Admire formation sandstone were two values, 0.044mg Ca⁺⁺/g rock and 0.071mg Ca⁺⁺/g rock, for samples from wells MP-130 and MP-110, respectively. INTERCOMP used an average of these values.

When only two values are available and these differ by a ratio of 1.6, it would seem reasonable to investigate further to determine an average value. However, it is doubtful, in the usual laboratory procedures of sample selection from cores, that an appropriate set of samples could be obtained for averaging which would reflect the combined effect of more permeable layers containing less clay but carrying more flow and the less permeable intervening shaly layers containing much more clay but carrying less flow. There are many such thin shaly layers in the Admire sandstone, particularly in the lower of the two main layers described elsewhere in this report. Transverse ion transport between layers only a few inches apart is certainly possible under the slow flow conditions existing over most of the distance between wells. The tendency in laboratory core sampling to avoid shale layers thus tends to minimize the indicated value of clay effects such as ion-exchange capacity and adsorption capacity (discussed later). With these considerations in mind, it is difficult to criticize INTERCOMP's decision simply to average the two data values available. It should be expected, however, that clay effects might well be considerably greater than this average would indicate.

(b) Cation Exchange Equilibrium Coefficient

With regard to the cation exchange equilibrium equation: the mass-action law equation or a surface double-layer equation attributed to Gapon (see discussion in Reference 9); based on the data available, there appears to be a preference for the mass-action type of equation, and INTERCOMP chose to use it and an equilibrium constant associated with it.

For the value of the constant INTERCOMP chose a value of 0.01. This was based on the data given in Reference 9. In that reference, data were given for the value of the equilibrium constant ranging from 0.0037 to 0.054 for different samples of Berea rock, and a value of 0.0143 for Tar Springs rock.

The equilibrium coefficient is the ratio of the square of the distribution ratio for monovalent cations to the distribution ratio for

divalent ions. The distribution ratio is the ratio of the concentration in clays to the concentration in adjacent solution, but expressed in appropriate units. Both INTERCOMP and Hill and Lake (Reference 9) used units of equivalents per liter of pore space (or milliequivalents per milliliter). If, for example, the monovalent ion concentration in solution is 0.0012 equivalents per liter and the divalent concentration is 0.000165 equivalents per liter, as indicated by Figures 20-23 of the INTERCOMP report, then if the monovalent ion concentration in the clays is one-tenth that in the aqueous phase or 0.00157 equivalent per liter of pore space, the divalent ion concentration (for a $K = 0.01$ is about 0.0274 equivalent per liter of pore space. This is about 165 times the amount present in the water per unit of pore volume. If the value of K were 0.05, this ratio would be cut to 155 (the monovalent ion concentration calculated to be present in clays is doubled). Thus, the reservoir of divalent ions present in the clays is not strongly affected by the choice of the value of the equilibrium coefficient.

It is concluded that the choice by INTERCOMP of a value of 0.01 for the equilibrium coefficient is appropriate and the exact value is not critical.

(2.) Non-Polymer Density and Viscosity Data B 1.1.6.

The data furnished by Cities Service Company in this classification were sufficient for simulation purposes. See, however, the discussion of micro-emulsion calculated viscosities, under B 1.1.4.

5.4.2 Interaction Descriptors

(1.) Oil-Water Relative Permeabilities and End-Point Versus Capillary Number B 1.1.2.

Oil-water relative permeability curves may be measured in the laboratory by established methods and such data were available from Cities Service Company for cores from wells MP-104, MP-124, and MP-217. The data for well 124 (the production well for the pattern being simulated) were used by INTERCOMP.

Such data show relative permeability behavior at very low capillary number ($N_c = u \mu / \sigma$). For a typical reservoir flow rate of one foot per day (0.00035 cm/sec), a water viscosity of 1.0 cp (0.01 g/cm/sec), and an interfacial tension in the usual range of about 35 dynes/cm (g/sec^2), the value of N_c is 1.0×10^{-7} . However, if a chemical slug is used instead of water to displace oil, the viscosity will be 10 times higher and the interfacial tension about 10,000 times lower, so that the value of N_c becomes about 10^{-2} . At this value of N_c the relative permeability curves, instead of being strongly concave upwards, become straight lines. Both the residual oil saturation and the connate water saturation decline to near zero values, and the relative permeabilities at the ends of the movable saturation range approach 1.0, so that the relative permeabilities of the phase are approximately equal to their volume fractions or saturations.

Data covering the way in which the relative permeability curves change with increasing capillary number are known as high-capillary-number relative permeability data. A complete set of such data (at a series of values of N_c) do not exist in the published literature. There are several publications^{3,8-40} that report measurements of residual oil saturation versus capillary number; the resulting curve is called a capillary desaturation curve. The minimum attainable water saturation decreases with increasing capillary number is also called a capillary desaturation curve. Only Gupta and Trushenski¹⁸ give both curves, and only for a single strongly water-wet Berea rock core.

Since chemical flooding is being applied as a supplemental oil recovery process only after extensive water-flooding has taken place, the reduction in residual oil saturation which accompanies the attainment of high capillary number is the mechanism by which the enhanced oil recovery is obtained. The change from very low capillary number (10^{-7}) to a high capillary number is a gradual process at any given point in the reservoir as the chemical slug approaches and passes the point. The change is primarily accomplished through interfacial tension reduction (only to a limited extent through the higher viscosity of the chemical slug) and because of dispersion the increase in concentration of surfactant and thus reduction in interfacial tension is gradual as the chemical slug approaches. It is necessary, therefore, that it be possible to calculate in a simulation the entire transition of the relative permeability curve shapes as well as the water and oil end-point saturations over the range from $N_c = 10^{-7}$ to $N_c = 10^{-2}$ or greater.

L. W. Lake has made a major contribution to the subject in Appendix D of the INTERCOMP report. He introduces the assumptions that the exponents of Corey-type relative permeability equations will decrease to 1.0 as the residual saturations decrease to zero in accordance with the capillary desaturation curve, and that the end-point relative permeability for a given phase will increase to 1.0 as the residual saturation of the other phase decreases to zero. With these assumptions, given a value of N_c and given capillary desaturation curves, it is possible to calculate values for the relative permeability of both the aqueous and the non-aqueous phase for any given aqueous phase saturation.

A major decision had to be made by INTERCOMP at this point. No capillary desaturation curves were available for the Admire sandstones. Furthermore, the Gupta-Trushenski curves for a strongly water-wet Berea core could not be accepted as applying directly to Admire sandstone, since it is known that the latter exhibits intermediate wetting (partly oil-wet). The Gupta-Trushenski curves for the wetting and non-wetting phases were displaced horizontally by about 3/4 of a log cycle. On the basis of the reasoning that intermediate wetting should lead to less separation of these curves, curves were arbitrarily drawn by INTERCOMP for Admire sandstone which have only 1/5 the horizontal separation of the Berea curves and lie about midway

between the Berea curves. This is shown as Figure 15 in the INTERCOMP report.

The Berea curves given by Gupta-Trushenski are not unique curves representing all strongly water-wet rocks. The capillary number $N_c = u\mu / \sigma$ is not the complete expression which represents the ratio of the viscous force tending to displace oil to the capillary force tending to retain it in waterflood residual form (disconnected ganglia blocked from moving by water films across pore throats). The remainder of this ratio is $(rl/2kk_{rw} \cos \theta)$, where r is the restraining pore throat radius, l is the ganglion length, k_{rw} is the relative permeability for the displacing phase, k is the rock permeability, and θ is the contact angle. For this part of the group to be dimensionless, the permeability k must be expressed in units of length squared, requiring permeability in darcys to be multiplied by 10^{-8} to obtain the permeability in cm^2 . Since ganglia will be displaced when the viscous/capillary force ratio reaches 1.0, but there is a distribution of values for (rl) for different ganglia, the average value of $(rl/2kk_{rw} \cos \theta)$ will be the reciprocal of the value of N_c when half of the residual oil is displaced. For Berea this occurs at $N_c = 10^{-4}$, hence $(\bar{r}l/2kk_{rw} \cos \theta) = 10$. If k is inserted in darcys, the value of the group is 10^4 divided by 10^8 , or 10^{-4} . The value of k was 0.677 darcy, k_{rw} was about 0.86 ($\approx S_w$ for half of S_{orw} of 0.28 displaced), and for the strongly water-wet condition, $\cos \theta = 1.0$. This would lead to an average value $(\bar{r}l)$ equal to about $0.86 \times 10^{-4} \text{ cm}^2$. If the average pore throat radius is derived from the permeability, porosity, and tortuosity by the Darcy-Poiseuille analogy, we obtain $\bar{r} \approx 7 \times 10^{-4} \text{ cm}$, which makes $\bar{l} \approx 0.12 \text{ cm}$. This does not seem unreasonable.

If the product $(\bar{r}l)$ is a constant times the permeability k for all rocks, then the Berea residual oil desaturation curve would be a unique curve applying to all rocks, requiring only to be shifted horizontally to the left for increasing values of the reciprocal of $\cos \theta$ (less strongly water-wet rock). That is, it should not require as large a value of N_c on the average to displace trapped oil ganglia from rocks of intermediate wetting ($\cos \theta < 1.0$).

We have no data which indicate that (rl/k) is a constant for all rocks, however, Therefore, use of the interpolated curves on Figure 15 to represent Admire sandstone is not supported by data, nor by a reasonable theory. Since the assumed curves are an essential part of the oil displacement calculation, this lack of support could be a significant weakness in the simulation effort.

It is only of practical effect, however, if the value of the capillary number N_c should be inadequate to displace oil in the simulations but large enough to actually do so in the reservoir, or vice versa. Since it is concluded here that the curve for Admire sandstone should be shifted to the left from the Berea curve, instead of to the right as was done by INTERCOMP, the effect is that it would be easier in the reservoir to displace residual oil than in the simulations. The INTERCOMP curve is therefore a pessimistic one and should not lead to over-optimistic predictions of oil recovery.

It is necessary to devise a way of predicting the relative permeability of the third (micro-emulsion) phase which appears between the aqueous and oil phases in the optimum region of water-phase salinity. The process must be designed so that this phase will appear, since the interfacial tension is lowest (and N_c highest) when this phase is present. Relative permeability data for this phase are not available. Lake, in Appendix D of the INTERCOMP report, has devised a way to construct a Corey-type equation for this phase from an interpolating function $g = S_o(1 - S_a)/(S_o + S_a)$ where S_o = oil phase saturation and S_a = aqueous or water phase saturation.

Lake's scheme for relative permeabilities has the attractive feature that it has all of the appropriate values at the limits and the functions all have appropriate shapes. There are no data to indicate that they are the correct shapes for Admire sandstone, however, except in the limit of very low N_c and only two phases present -- oil and water. These latter data are the only experimental data; all others are calculated on the basis of as-yet unverified assumptions. At the time that INTERCOMP undertook these simulations, it was necessary to proceed on the basis of Lake's model and assumptions.

In future cases, it would be desirable to secure at least a limited amount of data and attempt to confirm or if necessary modify Lake's model, since it represents an organizing principle for the representation of a large amount of relative permeability data (including desaturation) for simulation purposes.

INTERCOMP disregarded capillary pressure curves and their variation with interfacial tension. They concluded that capillary pressure was unimportant in this case. This is not a general conclusion. The process model includes the estimation of the interfacial tension in each grid block. It would be possible to multiply a standard oil-water capillary pressure curve by the ratio of the interfacial tension pressure difference for any given saturation and for each pair of phases.

(2.) Interfacial Tension Data B 1.1.3.

Some IFT data were available from Cities Service Company, but left much to be desired as a basis for making field predictions. This subject is well discussed in the INTERCOMP report.

What is not discussed in the INTERCOMP report is that the data represent two different IFT curves which cross in the region of optimal equivalent salinity, for any given surfactant concentration. These two curves are (a) the interfacial tension between oil phase and aqueous microemulsion phase, which decreases as the equivalent salinity increases from a low value, and (b) the interfacial tension between oleic microemulsion phase and aqueous or water phase, which decreases as the equivalent salinity decreases from a high value. The curves both persist in the region of salinity where a microemulsion phase exists between an oil phase and a water phase. The sum of the interfacial tension between water and microemulsion phase and the interfacial tension between

microemulsion phase and the oil phase must represent the interfacial tension between the water phase and the oil phase.

In the laboratory, because of density differences, the microemulsion phase settles out between the oil and water phase. During displacement in a rock formation, however, there is no reason why microemulsion phase must always intervene between oil and water phases and thus provide a lower interfacial tension in each interface. This being the case, from a conservative viewpoint the sum of the interfacial tensions would represent a pessimistic or conservative value to use in making displacement and oil recovery calculations. This was not done; rather, the larger of the two values was used.

It must be admitted that it will not generally be easy to determine, when three phases are present and flowing simultaneously, which phase is displacing the other two, or which interfacial tension (of the three which can be chosen) to use in calculating a capillary number and thus to calculate the relative permeability for each phase. It is apparent, however, that each interfacial tension would result in calculation of a different set of relative permeabilities via Lake's model. This discrepancy might be resolved by calculating an N_c for each pair of phases and then a relative permeability for one member of the pair from this N_c . This would require a corresponding modification of Lake's model.

(3.) Surfactant-Polymer Viscosity versus Concentration and Shear Rate Data B 1.1.4.

Discussion. As discussed in the INTERCOMP report, the relationship between polymer concentration, equivalent salinity, shear rate and viscosity which was available from Cities Service Company was satisfactory for the aqueous phase when it was not also the micellar phase. However, when oil is dispersed as a micellar solution in aqueous phase or vice versa in oil phase, or both together in a middle microemulsion phase, the linear-blending calculation of emulsion viscosity from oil and water viscosities as used by INTERCOMP is grossly in error. No data were provided by Cities Service Company. However, as INTERCOMP point out in retrospect, it would have been better to have used a correlation of literature data to predict microemulsion viscosity and its sensitivity to shear rate.

The low viscosities used for microemulsion phase by INTERCOMP lead to optimistic calculation of the displacement rate of this phase (or to too low a pressure gradient in a region where it is the principal flowing phase).

(4.) Salinity Requirement Diagram B 1.1.5

Discussion. At this point in the process model, another general mathematical model, in this case of equilibrium phase relationships, is introduced by INTERCOMP. It is described in the public literature^{4 1, 4 2} and in Appendix C of the INTERCOMP report. The general model contains a large number of parameters^{4 3} which

enable the two-phase regions to have skewed rather than symmetrical shapes, which determine the size of the two-phase regions (area relative to triangle in a triangular diagram), the locations of plait points, the relationship between points at the two ends of tie-lines in the two-phase regions, and the location of the three points enclosing a three-phase region, when such a region exists. Further, the mathematical model enables the calculation of the change in these relationships as the equivalent salinity varies.

INTERCOMP used a simplified version of this model to represent the chemical system and crude oil behavior in the El Dorado field, because insufficient data on phase behavior were available from which to calculate or estimate all of the parameters affecting the calculated phase behavior. The simplifications reduced the number of parameters to seven.

Two forms of data were obtained from Cities Service Company: (a) Phase Volume Data and (b) Salinity Requirement Diagrams. The phase volume data were provided as tables giving the volume observed of upper phase, lower phase, and middle phase (if it existed) in a series of experiments with 1:1 ratio of oil and water with (for each table) a fixed surfactant content but varying salinity of the water. These data are plotted in Figures 1, 2, 3, and 4 of the INTERCOMP report. These diagrams should have relatively smooth curves of the shapes shown in Figure 15, Reference 15. The curves of Figures 1 to 3 are for the most part irregular in shape, and it is difficult to determine the equivalent salinity at which the phase behavior changes from Type II (-) to Type III and the salinity of the change from Type III to Type II (+). These are critical parameters in the Pope-Nelson phase behavior model. When the curves are smooth it is also possible to estimate with reasonable accuracy the height of the two-phase region in the Type II (-) and Type II (+) systems, and the height of the middle point of the triangular three-phase region in the Type III system. The two salinities and the three heights are five of the parameters used by INTERCOMP. The other two are the locations of the plait point in Type II (-) and Type II (+) systems. These were arbitrarily estimated on the basis of experience with a similar chemical system and other crude oils.

The salinity requirement diagrams furnished by Cities Service Company are shown in Figure 6 of the INTERCOMP report. Two diagrams are given, for different ratios of calcium to sodium in the brine. The shaded areas represent salinity intervals where the phase behavior is Type III (lowest interfacial tension) and so are labelled optimal salinity regions. The optimal salinity region varies moderately with surfactant concentration and strongly with the calcium content of the brine. The calcium/sodium weight ratio in the El Dorado reservoir is about half way between the values of 0.0 and 0.22 for which optimal salinity regions are shown. INTERCOMP, therefore, interpolated between the two diagrams. At high surfactant concentration on this diagram, representing conditions in the reservoir near the injection well, the lower salinity is approximately 1%w NaCl, and the high about 1.5%w NaCl. As the slug is dispersed, diluted, and reduced in amount by adsorption on

the rock, the surfactant concentration decreases. At one-fourth of the maximum concentration on the diagram, the interpolated lower and upper salinities would be about half the values at the maximum surfactant concentration.

INTERCOMP's mathematical model did not allow this variation of optimum salinity range with change in surfactant concentration; they used, therefore, constant lower and upper salinity bounds for the optimal salinity region. This lack in the model was later corrected but had certain consequences in the El Dorado simulations: as the surfactant concentration decreases, the simulation continues to calculate a Type III region to exist at a high salinity than that at which the phase behavior would actually change to Type II (+); the latter condition is unfavorable (surfactant moving slower than calculated). When the salinity is lower than the constant lower value assumed for the Type III region, the phase behavior is calculated to be Type II (-) when it still may be Type III, and again the surfactant is likely to be actually moving more slowly than is calculated in the simulation.

In simulations of the pilot area, INTERCOMP found it necessary to reduce greatly the value of the lower salinity bound of the Type III region of phase behavior in order to match the transport rate of the surfactant. Good reasons may be deduced for this change, as stated by INTERCOMP.

A better basis for calculating the parameters of this phase-behavior model should be provided in future cases. The phase-behavior mathematical model seems adequate for simulation purposes, if provided with good data from which most of the parameters may be calculated.

5.4.3 Coreflood Performance

- (1.) Process Requirements:
 - B 1.4.1 Coreflood Design
 - B 1.4.2 Coreflood
 - B 1.4.3 Coreflood Performance Data

Discussion. Cities Service Company had performed a considerable number of corefloods of a screening nature⁴⁴. Only oil cut versus throughput, oil recovery, and surfactant recovery were reported (no surfactant, co-surfactant, or polymer profiles, no monovalent and divalent ion profiles). Only one coreflood was reported using the chemical system which was employed in the field-scale pilot test.

INTERCOMP matched the available data on this coreflood by raising slightly the lower-bound salinity for the three-phase region of phase behavior. This is actually in accord with the surfactant concentration used in the coreflood, which was 0.085 meq/ml as compared to the upper limit of concentration on Figure 6 of 0.075 meq/ml, and also with the fact that the calcium/sodium ratio was considerably lower (0.0044) than the ratio for the field. The result

was a Type II (-) phase behavior. The interfacial tension was adequately low under the conditions of the core test to give a good oil recovery, and surfactant was transported in the aqueous phase and recovered in the simulation in amount similar to that in the lab test.

INTERCOMP did not consider this single coreflood to be an adequate test of the process model, and so they did only a few one-dimensional simulations under the coreflood conditions to test the sensitivity of the calculated oil and surfactant recovery to changes in a single variable: the input surfactant adsorption level (which was derived by matching the surfactant recovery in the coreflood under Type II (-) phase behavior conditions).

Polymer adsorption data for use in pilot simulations should be derived from corefloods, but since no polymer effluent curves were available, INTERCOMP simply assumed typical values for polymer adsorption and for the pore volume fraction of the rock which is inaccessible to polymer molecules. These data (along with phase behavior) control the calculated transport behavior of polymer in the reservoir. No conclusions can be drawn from an apparent match of polymer transport rate, such as that shown in Figures 25, 27, and 30 of the INTERCOMP report other than that the combination of assumed data worked out about right (the individual assumed data are not each confirmed thereby).

It would certainly be preferable in future cases to have results of coreflood tests available in which effluent profiles of all system components are obtained, together with pressure drop data at a fixed flow rate, and a series of such tests to have the major variables changed through two or three levels (including flow rate).

A longitudinal dispersion coefficient in the form of a mixing length, $\alpha_L = D_{eff}/u$, is used in the INTERCOMP simulator. Values of this parameter may be obtained from laboratory corefloods, but more reliably from field test data. INTERCOMP used a value obtained by analysis of salinity changes at observation wells in the El Dorado pilot.

The simulator also uses a value of the transverse mixing length, α_t , when more than one layer is present, to account for dispersive crossflow between layers. A low value of 0.005 ft was used.

INTERCOMP concluded on the basis of comparing two-layer with one-layer simulations that even with this low value of α_t , the two layers behaved very similarly to one layer. Hence, they discarded the two-layer model of the reservoir furnished by GURC and proceeded to do the rest of their simulation work with one layer. They quote calculations by Lake based on some of the pilot data which support their conclusion.

It must be mentioned, however, that layer pilot data⁴⁵ indicate a separate arrival of chemical slug and oil bank in the lower layer at the observation wells. This implies that the layers are not in good

communication with each other in the pilot area, as must have been supposed by Lake and as indicated by the vertical permeabilities about equal to one-eighth of the horizontal permeabilities, as given in Tables 6 and 7 of the INTERCOMP report. It may be that the shale layers in the upper part of the lower layer are more continuous than they were previously thought to be.

The apparent similarity of INTERCOMP's one- and two-layer simulations may also be due in part to a combination of numerical dispersion (with only 20 blocks in the longitudinal direction in the field-scale simulations of the center stream-tube) with the longitudinal dispersion contributed by α_L . If the profiles in each layer are sufficiently stretched out by each dispersion, they will not look very different, and indeed a single layer with that much dispersion may give equivalent results. This may be a faithful reflection of field process behavior.

Another aspect of process behavior which is evident from the observed well logs but not from INTERCOMP's simulations is the tendency toward gravity segregation in each layer. The oil phase is lighter than the aqueous phase and the microemulsion phase. Over short vertical heights such as in the El Dorado reservoir, oil-water capillary pressure combined with viscous force tends to make oil and water saturations nearly uniform over the layer height. In a chemical flood, however, the capillary pressure is reduced near to zero as the interfacial tension falls to values well below one dyne per centimeter. Under these circumstances, gravity segregation should be a significant effect. The saturation changes accompanying this segregation will affect relative permeabilities and transport rates. The gravity segregation effects can only be observed in simulations if more than one layer is used and the capillary pressure curves and their alteration as interfacial tension changes are included in the process model. Since the two layers at El Dorado apparently do not communicate as well as was thought, the segregation will occur within each layer (as was indicated by the observer well logs). To observe this effect in simulations would require the use of two or more layers to represent each of the two stratigraphically defined layers.

There is, thus, room for improvement in future simulations of El Dorado and other similar chemical flooding projects.

6.0 SUMMARY

The numerical modeling and simulation conducted by Cities Service Company in the El Dorado project, or any operator for their own purposes on their own lease, is not subject to question; however, the availability of data from the Federal-industry joint-venture program is public concern. This study defines the specific data sets that GURC believes are necessary to characterize a surfactant-polymer project such as El Dorado.

The conclusion of the study is that data in the public domain are not adequate for simulation, even when "public domain" is defined to include all data sources reasonably available to a knowledgeable, good-faith operator, in addition to Federal reports and professional publications.

A major factor in the discrepancies between simulation and field performance is insufficient characterization of the reservoir with geologic and with fluid/rock descriptors. Those characterizations should be sufficiently accurate in the first place that remedial capacities of sensitivity runs can, thereafter, accomplish all necessary adjustments within cost-effective limits.

Geologic characterization requires a number of rock and fluid/rock system descriptors, both qualitative and quantitative, beyond customary practices. These are defined in Sections 4.2.1 and 4.3.1. The principal deficiency, and basic source of simulation failure with respect to reservoir and fluid/rock characterization, results from the effects of physical and chemical heterogeneities. This deficiency can be overcome in large degree by fulfilling the data requirements defined in Sections 4.2.2, 4.2.3, and 4.3.2.

A relatively small but influential body of literature exists, evolved from research in recent sediments by industry, first, and academia, second, which defines generic depositional models and their internal characteristics. This specialized body of geological knowledge can be used to achieve order in the use of disparate field data and to extend quantified borehole measurements between and beyond the points of well control.

The simulation program did not produce acceptable results for technical or economical forecasting. The best match was at observation well MP-131 but great disparity existed even there between predicted and actual oil cut behavior. Whether a history match was achieved at any point in the reservoir is questionable.

Verification of the chemical process description was based on data from one well, and that well had a limited sampling interval that was not representative of the amount of surfactant in the oil phase in the reservoir.

The simulation program placed much emphasis on phase equilibrium, but input inaccurate data in the CSEL and CSEU phase volume plots and indeterminable salinity requirement values.

Perhaps most critical in principle, sensitivity studies were minimized despite the lack of history match, resulting in isolating the simulation from the real world.

The project shows that the data required for input to a state-of-the-art chemical flooding simulator are both voluminous and complex. Data which are in the public

domain need to be supplemented by a large amount of other data, both geologic and physico-chemical in nature. At best, some process data must be assumed while research continues in the universities and companies; however, none can be neglected or misused if, as exemplified in this study, we are to understand how a pilot project performs reasonably well in some aspects or why it does not perform in others.

REFERENCES CITED

- 1 Parke A. Dickey, Petroleum Development Geology, 2nd edition 1981, PennWell Publishing Co., Tulsa, Oklahoma, 428 p.
- 2 J. R. Crump, E. L. Claridge, and R. D. Young, 1981, Chemicals for chemical flooding in enhanced oil recovery, GURC for U.S. Department of Energy, rept. DOE/ET/10145-66.
- 3 E. L. Secrest and J. W. Jones, 1981, A computer model for comparative economic analysis of enhanced oil recovery projects, GURC for U.S. Department of Energy, rept. DOE/ET/10145-69.
- 4 B. C. Craft and M. F. Hawkins 1959, Applied petroleum reservoir engineering, Prentice-Hall, Inc., Englewood Cliffs, N.J., 437 p.
- 5 Henry B. Crichlow, 1977, Modern reservoir engineering, a simulations approach, Prentice-Hall, Inc., Englewood Cliffs, N.J., 354 p.
- 6 R. F. Monicard, 1980, Properties of reservoir rocks: core analysis, Gulf Publishing Co., Houston, Texas, 168 p.
- 7 Robert R. Berg, 1979, Geologic characterization of Admire reservoir sandstone project, Butler County, Kansas, in Jensen and Zimmerman, 1981.
- 8 *ibid.*
- 9 _____, 1980, El Dorado micellar-polymer pilot, data assessment and numerical simulation, INTERCOMP report to GURC with appendices, Appendices II and III to this report in separate vols.
- 10 Donald F. Zetik, 1976, Reservoir simulation for the El Dorado micellar-polymer project, SPE paper number 5807, SPE Symposium in improved oil recovery, Tulsa, Okla., March 22-24, 1976.
- 11 GURC file on non-attribution basis.
- 12 *ibid.*
- 13 Berg, 1979 (Reference 7).
- 14 J. F. Tomich, R. L. Dalton, Jr., H. A. Deans, and L. K. Shallenburger, 1973, Single-well tracer method to measure residual oil saturation, Jour. Pet. Tech., Feb. 1973, p. 211-218.
- 15 R. E. Wyman, H. A. Deans, and E. H. Koepf, Determination of residual oil saturation, publ. by Interstate Oil Compact Commission, P. O. Box 53127, Okla. City, Okla. 73152. Ch. V by Wyman gives logging methods. Ch. VII by Deans describes the single well tracer test. Ch. VIII by Koepf describes the pressure core technique. Other chapters describe indirect methods.

- 16 H. L. Stone, 1973, Estimation of three-phase relative permeability and residual oil data, Jour. Cdn. Pet. Tech., Oct. 1973, No. 4. Also, Probability model for estimating three-phase relative permeability, Jour. Pet. Tech., Feb. 1970.
- 17 J. K. Dietrich, 1976, Three-phase relative permeability models, SPE paper number 6044 presented at the SPE Annual Meeting, New Orleans, Oct. 3-6, 1976.
- 18 S. P. Gupta and S. P. Trushenski, 1979, Micellar flooding — compositional effects on oil displacement, Soc. Pet. Engr. Jour., April 1979, p. 116-128.
- 19 A. Abrams, The influence of fluid viscosity, interfacial tension, and flow velocity on residual oil saturation left by waterflood, Soc. Pet. Engr. Jour., Oct. 1975, p. 435-447.
- 20 R. B. Lantz, 1971, Quantitative evaluation of numerical diffusion (truncation error), Soc. Pet. Engr. Jour., Sept. 1971, p. 315.
- 21 M. R. Todd, P. M. O'Dell, and G. J. Hirasaki, 1972, Methods for increased accuracy in numerical reservoir simulators, Soc. Pet. Engr. Jour., Dec. 1972, p. 515-530.
- 22 M. R. Todd and C. A. Chase, 1979, A numerical simulator for predicting chemical flood performance, SPE paper number 7691 presented at SPE Fifth Symposium on reservoir simulation, Denver, Jan. 31-Feb. 2, 1979.
- 23 T. K. Perkins and D. C. Johnston, 1963, A review of diffusion and dispersion in porous media, Soc. Pet. Engr. Jour., Mar. 1963, p. 70.
- 24 M. H. Waxman and E. C. Thomas, 1968, Electric conductivities in shaly sands, Jour. et. Tech., Feb. 1974, p. 213. Waxman and L. J. M. Smits, 1968, Electrical conductivities in oil-bearing shaly sands, Soc. Pet. Engr. Jour., June 1968, p. 107.
- 25 M. M. Mortland and L. L. Mellor, 1954, Proc. Soil Sci. Soc. Amer., 363 p.
- 26 Ralph E. Grim, 1968, Clay mineralogy, McGraw-Hill.
- 27 H. J. Hill and J. D. Milburn, 1956, AIME Trans., vol. 207, p. 65.
- 28 Waxman and Smits, 1968 (Reference 24).
- 29 E. C. Thomas, 1976, Jour. Pet. Tech., Sept. 1976, p. 1087.
- 30 L. W. Holm and V. A. Josendal, 1972, O&G Jour. Nov. 13, 1972, p. 158.
- 31 G. G. Bernard, 1975, Jour. Pet. Tech., Feb. 1975, p. 179.
- 32 H. J. Hill, F. G. Helfferich, L. W. Lake, J. Reisberg, and G. A. Pope, 1977, Jour. Pet. Tech., Oct. 1977, P. 1336.
- 33 F. W. Smith, 1978, Jour. Pet. Tech., June 1978, p. 959.
- 34 G. A. Pope, L. W. Lake, and F. G. Helfferich, 1978, Soc. Pet. Engr. Jour., Dec. 1978, p. 418.
- 35 L. W. Lake and F. G. Helfferich, 1978, Soc. Pet. Engr. Jour., Dec. 1978, p. 435.

- 36 H. J. Hill and L. W. Lake, 1978, Soc. Pet. Engr. Jour., Dec. 1978, p. 445.
- 37 Mortland and Mellor, 1954 (Reference 25).
- 38 J. J. Taber, 1969, Soc. Pet. Engr. Jour., March 1969, p. 3.
- 39 A. Abrams, 1975, Soc. Pet. Engr. Jour., Oct. 1975, p. 437.
- 40 Gupta and Trushenski, 1979 (Reference 18).
- 41 G. A. Pope and R. C. Nelson, 1978, Soc. Pet. Engr. Jour., Oct. 1978, p. 339.
- 42 G. A. Pope, Ben Wang, and K. Tsaur, 1979, Soc. Pet. Engr. Jour., Dec. 1979, p. 357.
- 43 ibid.
- 44 G. E. Kellerhals, 1979, SPE paper number 8197, presented at SPE 1979 fall meeting, Las Vegas, Nevada.
- 45 _____, 1981, Improved oil recovery by micellar-polymer flooding, El Dorado field, Kansas, monthly report for May 1981. DOE/ET/13070-72.

GLOSSARY

In so far as they cover the subject area, symbols in this report are in accord with the Standard Letter Symbols of SPE for Petroleum Reservoir Engineering. Where extension of the symbols has been required, the additions have been made consistent with SPE Standards. Common scientific and engineering symbols have not been included.

Symbols and Symbols-Subscripts in Alphabetical Order

English

B

- B_o formation volume for oil, reservoir barrels per stock tank barrel
 B_g formation volume for gas, reservoir cu. ft per standard cu. ft
BHP bottomhole pressure, psi

C

- C^+ concentration of monovalent ion in solution, meq/ml
 C_r^+ concentration of monovalent ion on rock, meq/gr
 C^{++} concentration of bivalent ion in solution, meq/ml
 C_r^{++} concentration of bivalent ion on rock, meq/gr
Ca calcium ion
 C_μ pressure coefficient of viscosity
c compressibility

D

- D_{eff} effective diffusion coefficient

F

- FVF formation volume factor for oil, reservoir barrels per stock tank barrel
F formation resistivity factor

G

- GOR gas-oil ratio

H	
h	formation thickness
K	
k	permeability, millidarcys
k_g	permeability to gas
k_o	permeability to oil
k_w	permeability to water
k_{ro}	relative permeability to oil
k_{rw}	relative permeability to water
K	mass-action equilibrium constant
K_L	longitudinal dispersion coefficient
K_t	transverse dispersion coefficient
M	
meq	milliequivalents
N	
n	saturation exponent
N_c	capillary number
P	
P	pressure
Q	
Q	ion exchange capacity
R	
R	resistivity (electric logging)
R_o	resistivity of rock sample saturated with brine
R_s	solution GOR
R_t	resistivity of the partly oil-saturated, partly brine-saturated rock
R_w	resistivity of brine
\bar{r}	average pore radius
$\bar{r}l$	average pore radius times ganglion length

S

S_g	gas saturation
S_{gc}	critical gas saturated
S_o	oil saturation
S_{oi}	initial or original oil saturation
S_{or}	residual or remaining oil saturation
S_{org}	residual oil saturation from gas flooding
S_{orw}	residual oil saturation from water flooding
S_w	water saturation
S_{wc}	connate water saturation

U

u	velocity
-----	----------

V

V	volume
-----	--------

Greek α

α_L	longitudinal dispersive mixing length
α_t	transverse dispersive mixing length

 μ

μ	viscosity
μ_g	viscosity of gas
μ_o	viscosity of oil
μ_w	viscosity of water

 ρ

ρ	density
--------	---------

 σ

σ	surface tension
----------	-----------------

 τ

τ	tortuosity
--------	------------

 ϕ

ϕ	porosity
--------	----------